Dependence of behavioral and neocortical seizures on brain pH and oxygen levels in a rat model of term birth asphyxia

Tommi Ala-Kurikka[1,2], Alexey Pospelov[1,2], Milla Summanen[1,2], Aleksander Alafuzoff[1,2], Juha Voipio[1], Kai Kaila[1,2]

1. Faculty of Biological and Environmental Sciences, Molecular and Integrative Biosciences, University of Helsinki, 00014 Helsinki, Finland.

2. Neuroscience Center (HiLIFE), University of Helsinki, 00014 Helsinki, Finland.

Correspondence:
Kai Kaila
Faculty of Biological and Environmental Sciences
Molecular and Integrative Biosciences
PO Box 64
00014 University of Helsinki
Finland
Email: kai.kaila@helsinki.fi
Phone: +358 2941 59860

ABSTRACT

Birth asphyxia (BA) is a pathologic condition that arises from severe perinatal hypoxia and hypercapnia. Recovery following BA is often associated with seizures which may exacerbate the ensuing hypoxic-ischemic encephalopathy (HIE). Drugs used to treat post-BA seizures are often ineffective and there are concerns over their safety. Therefore, novel seizure-suppressing therapies are urgently needed. Most rodent models of BA-induced seizures are based on exposing neonatal rats or mice to hypoxia (or hypoxia-ischemia), and overlook the fact that the hypercapnic acidosis linked to asphyxia has brain-sparing effects by suppressing neuronal excitability and enhancing cerebral blood flow. Thus, the aim of the present study was to investigate the dependence of asphyxia-induced seizures on brain pH and oxygen (Po_2) levels in a rodent model of term BA based on postnatal day 11-12 rat pups. Cortical activity and electrographic seizures were recorded in freely-behaving animals using epidural electrodes. Simultaneous measurements of cortical local field potentials as well as intracortical pH and Po_2 were made using microelectrodes and microsensors in urethane-anesthesized animals. The pups were exposed either to steady asphyxia (duration 15 min; with ambient air containing 5 % O_2 plus 20 % CO_2) or to intermittent asphyxia (30 min; with repetitive 5 min steps from 9 % to 5 % O_2 at constant 20 % CO_2). Both protocols led to acidemia (blood pH <7.0) coupled to a fall in base excess by 20 mmol/l, and to a large increase in plasma copeptin (from 0.2 nM to about 5 nM), a biomarker of BA. Brain pH decreased from 7.3 to 6.7 by the end of intermittent asphyxia. Brain Po_2 was only transiently affected by 9% ambient O_2, but it fell below the level of detection with steps

to 5 % O_2, during which neuronal activity was near-abolished. The Po_2 steps to 9% were associated with a moderate increase in pH (0.12 units) and a slight recovery (~10 % of baseline) in ongoing neuronal activity. Behavioral seizures spanning the entire Racine scale were triggered after intermittent but not steady asphyxia, and they were tightly associated with neocortical electrographic seizures. The seizures were strongly suppressed when the post-asphyxia brain pH recovery was slowed down by a low level (5 %) of ambient CO_2. The post-asphyxia overshoot in brain Po_2 (from 30 to 85 mmHg) had no discernible effect on neuronal activity. Our data suggest that the recurring hypoxic episodes during intermittent asphyxia promote neuronal excitability, which becomes established as hyperexcitability and seizures once the suppressing effect of the hypercapnic acidosis is relieved. The present rodent model of BA is to our best knowledge the first one where, consistent with the clinical picture of BA, robust behavioral and electrographic seizures are triggered after and not during the asphyxic insult.

HIGHLIGHTS

- Experimental asphyxia induced severe acidemia and abolished most cortical activity.
- Cortical activity during asphyxia was closely linked with changes in brain pH but not Po_2.
- Behavioral and electrographic seizures were triggered after intermittent asphyxia.
- Behavioral convulsions were closely associated with electrographic seizures.
- The post-asphyxia seizures were suppressed when brain pH recovery was slowed down with 5 % CO_2.

KEYWORDS

perinatal asphyxia; neonatal seizures; hypoxia; hypercapnia; copeptin; vasopressin; neuroprotection; chemoreflex; brain-sparing; resuscitation

INTRODUCTION

During mammalian birth, the fetus is exposed to a period of asphyxia when the umbilical exchange of respiratory gases (O_2 and CO_2) is halted, and lung-based breathing takes over. The asphyxia triggers a wide range of adaptive responses, which are necessary for the fetus to cope with the transient reduction of oxygen availability and which facilitate the subsequent adjustment to extrauterine life (Evers and Wellmann, 2016; Giussani, 2016; Lagercrantz, 2016; Lear et al., 2018; Rainaldi and Perlman, 2016; Spoljaric et al., 2017). While numerous beneficial effects of the “obligatory asphyxia” are associated with normal birth, prolonged perinatal asphyxia caused by complicated birth is harmful to the neonate. Thus, the clinical diagnosis of birth asphyxia (BA) refers to a pathologic condition of the neonate arising from a prolonged

perinatal impairment of respiratory gas exchange (Sanders et al., 2010). Severe BA is one of the leading causes of neonatal mortality resulting in around one million neonatal deaths annually (Lawn et al., 2005). In survivors, BA leads to hypoxic-ischemic encephalopathy (HIE) making them prone to a wide variety of developmental aberrations and lifelong malfunctions of the brain, ranging from minor and major psychiatric and neurological disorders to cerebral palsy (Ahearne et al., 2016; Dalman et al., 2001; Modabbernia et al., 2016; Pappas and Korzeniewski, 2016; Rosso et al., 2000).

The period of recovery after asphyxia is often marked by seizures, some of which are considered to promote HIE-related trauma (Bennet et al., 2007; Glass et al., 2009; Kharoshankaya et al., 2016; McBride et al., 2000; Miller et al., 2002; Pressler and Mangum, 2013; Soul et al., 2019; van Rooij et al., 2010; Wirrell et al., 2001). Suppression of seizures has been notoriously unsuccessful with current pharmacological approaches. Notably, there are no clinical follow-up studies that would provide evidence for improved long-term outcomes in post-BA infants, who have received anticonvulsant drug therapy after birth. On the contrary, a large number of preclinical studies suggest that many anticonvulsants used in the neonatal intensive care unit (NICU) may have deleterious actions on the developing brain (Bittigau et al., 2002; Ikonomidou and Turski, 2010). Thus, designing novel approaches to suppress neonatal seizures is an unmet and urgent goal (Pressler and Lagae, 2019; Soul et al., 2019).

Large-animal models have numerous advantages with regard to instrumentation and multimodal monitoring in studies on adaptive and pathophysiological mechanisms associated with BA (Drury et al., 2015; Hassell et al., 2015; Saugstad et al., 2019). On the other hand, standard laboratory rodents offer the potential for implementing a vast array of current neurobiological techniques for translational work. Unfortunately, however, practically all preclinical models on BA which employ neonatal rodents, are based on exposure of the animals to hypoxia or hypoxia-ischemia (Jensen et al., 1991; Rice et al., 1981; Sun et al., 2016; Vannucci and Vannucci, 2005).

By definition, asphyxia is a combination of systemic hypoxia and hypercapnia, and these two components of asphyxia have distinct – often functionally opposite – actions on the brain. Indeed, while hypoxia as such is known to promote neuronal excitability and seizures (Kawasaki *et al.*, 1990; Jensen *et al.*, 1991; Peng *et al.*, 2013; Sampath *et al.*, 2014; Zanelli *et al.*, 2014 and references below), an elevation of systemic CO_2 produces a fall in brain pH and a consequent decrease in neuronal excitability (Lee et al., 1996; Pasternack et al., 1996; Ruusuvuori and Kaila, 2014; Schuchmann et al., 2006; Shi et al., 2017; Tolner et al., 2011). Moreover, a rise in CO_2 leads to vasodilation of cerebral arteries and arterioles (Giussani, 2016; Vutskits, 2014) and, acting in synergy with neurohormonal factors such as vasopressin (Perez et al., 1989), mediates a brain-sparing increase in cerebral blood flow and oxygenation during the asphyxia-coupled reduction of O_2 availability (Giussani, 2016). The mismatch between hypoxia-based preclinical models and human BA is

clearly evident from observations that, in such models, seizures are triggered *during* the exposure to hypoxia (Jensen et al., 1991; Sampath et al., 2014). This is in stark contrast with the fact that seizures in human neonates are triggered *after* a period of moderate or severe asphyxia (Lynch et al., 2012).

The aim of the present study was to investigate the dependence of seizure generation on changes in brain pH/CO_2 and oxygen levels in the rat model that we have recently used to study hormonal and brain-protective responses in asphyxiated rodents (Pospelov et al., 2020; Summanen et al., 2018). This model replicates the most fundamental features of BA in human neonates. We used postnatal-day (P) 11-12 rats which, in terms of cortical development, are at a stage that is equivalent to the human term neonate (Clancy et al., 2007; Romijn et al., 1991; Semple et al., 2013). Asphyxia was induced by ambient gas mixtures containing 5 % or 9 % O_2 and 20 % CO_2 (balanced with N_2). Two protocols were used in the present study: *steady asphyxia* (5 % O_2 plus 20 % CO_2) which mimics an acute complication such as placental abruption or maintained cord compression; and *intermittent asphyxia* where the hypoxia is applied in repetitive steps at 9 % O_2 and 5 % O_2 (at constant 20 % CO_2) in order to roughly mimic the effects of recurring contractions during prolonged parturition. The mechanisms underlying the changes in brain and subcutaneous pH and O_2 levels in this model have been recently described under seizure-free conditions achieved using anesthesia and a slightly lower body temperature (Pospelov et al., 2020).

As shown here, the present model fulfills the main diagnostic criteria of BA in terms of blood acid-base parameters (American Academy of Pediatrics and American College of Obstetricians and Gynecologists, 2014). Moreover, a large release of copeptin, which is a stable fragment of pre-proAVP and a tell-tale blood biomarker of BA (Kelen et al., 2017; Schlapbach et al., 2011; see also Wellmann et al., 2010), was seen in response to asphyxia. In sharp contrast to all BA models based on hypoxia only, seizures were never observed during the profound brain hypoxia which takes place during exposure to asphyxia with 5 % O_2. However, we observed intense behavioral convulsions, which were tightly linked to electrographic cortical seizures, during brain pH recovery after the intermittent asphyxia protocol. From a therapeutic point of view, an interesting observation was that the seizures were abolished or strongly suppressed when the rate of post-asphyxia brain pH recovery was slowed down by applying a low level (5 %) of ambient CO_2. No seizures were seen after steady asphyxia. This striking difference in seizure propensity following the steady and intermittent asphyxia protocols suggests that periodic hypoxic episodes in the asphyxic brain enhance neuronal excitability (Jensen and Wang, 1996; Quintana et al., 2015; Zanelli et al., 2015), which becomes established as hyperexcitability and seizures once the suppressing effect of the asphyxia-related hypercapnic acidosis is relieved. This scenario would readily explain why BA seizures in human neonates take place *after*, but not during parturition. As a whole, our work indicates brain pH as an accessible target for therapeutic maneuvers aiming at suppression of neonatal seizures following BA.

MATERIALS AND METHODS

Animals

Experiments were performed using postnatal day (P) 11-12 male Wistar Han rats (*n* = 166). The animals were maintained in the Laboratory Animal Centre of the University of Helsinki in an in-house animal facility under 12-hour light/dark cycle (lights on at 6 am) with a temperature and relative humidity of 21-23 °C and 45-55 %, respectively. Water and food (Altromin 1314 Forti, Lage, Germany) was available *ad libitum*. All experiments were carried out in accordance with the ARRIVE guidelines and the European Union Directive 2010/63/EU on the protection of animals used for scientific purposes. They had been approved by the National Animal Ethics Committee of Finland, and the Animal Ethics Committee of the University of Helsinki. A maximum of two animals per litter were used, and littermates were never included in a given experimental group.

Experimental asphyxia

The rat pups were placed in a 2000 ml chamber heated to 36 °C 30-45 min prior to exposure to asphyxia. All gases were humidified and warmed, and delivered to the chamber at 2000 ml/min. We have found that under these conditions the animals' rectal temperature stabilizes to 36.5 – 37.0 °C. The asphyxia and hypercarbia gasses were either premixed and bottled by AGA (Espoo, Finland) or were mixed on-site using an Environics S4000 gas mixing system (Tolland, Connecticut, USA).

Two distinct asphyxia protocols, steady asphyxia and intermittent asphyxia, were used to simulate BA arising from acute complications such as placental abruption or maintained cord compression and the effects of recurring contractions during prolonged parturition, respectively. In steady asphyxia, the animals were exposed to 5 % O_2 / 20 % CO_2 (balanced with N_2) for 15 min after which they were promptly re-exposed to room air and monitored for up to 90 min. The intermittent asphyxia consisted of 20 % CO_2 with three alternating 5 min periods of 9 % O_2 and 5 % O_2 exposures, with a total duration of 30 min (see Fig. 1). After the intermittent asphyxia, the first 30 min of recovery occurred either in room air (rapid restoration of normocapnia, RRN) or in 21 % O_2 / 5 % CO_2 gas (graded restoration of normocapnia, GRN) and was followed by 60 min in room air. Rats in the control group were kept in the experimental chamber, in room air, for an equivalent time.

Blood sample collection

After asphyxia (or room air in controls), the animals were decapitated, and 80 µl of blood was collected straight from the trunk into lithium heparin coated plastic capillaries for blood-gas measurements. The rest

of the trunk blood was collected into EDTA-coated tubes and protease inhibitors (Complete, Roche) were added. The samples were centrifuged 10 min at 1300 g in 4 °C. Plasma samples were stored at -80 °C and analyzed within 2 months of collection.

Blood-gas and copeptin measurements

Blood pH, Pco_2 and lactate were measured from the trunk blood using a GEM Premier 4000 Blood-gas analyzer (Instrumentation Laboratory, Lexington, Massachusetts, USA). Base excess (BE) was calculated from pH and Pco_2 as described in Summanen *et al.* (2018). The analyzer is designed to detect pH ≥ 6.8 and Pco_2 ≤ 20 kPa. 1/5 and 2/5 animals sampled immediately after intermittent and steady asphyxia, respectively, had blood pH lower and a Pco_2 higher than these limits. For the purpose of calculating BE, pH was assumed in these cases to be 6.8 and Pco_2 to be 20 kPa. The BE for these animals was -11.2 mmol/l. Notably, the median values of the data in Fig. 1 will not be affected by this (statistically conservative) approximation.

Copeptin concentrations in rat plasma were measured using an assay based on AlphaLISA (PerkinElmer) as previously described (Summanen et al., 2018). In brief, 5 µl of blank, sample or standard (0-160 ng/ml) solution was pipetted in triplicate on a 384-well AlphaPlate. 10 µl of goat anti-copeptin (SantaCruz Biotechnology) conjugated to AlphaLISA acceptor beads (20 µg/ml) was added to each well. The plate was incubated for 1 h before adding 10 µl of 5 nM biotinylated sheep anti-copeptin (Thermo Scientific) and, after another 1 h incubation, 25 µl of streptavidin-coated AlphaLISA donor beads (40 µg/ml) to each well. After a final 1 h incubation, the plate was read with an EnSpire Alpha plate reader (PerkinElmer). The standard curve was calculated with GraphPad Prism software (San Diego, California, USA) using 4-parameter logistic regression.

Behavioral seizure scoring

Animals were recorded during the experiments using either a Sony HDR-CX410 or a Logitech C310 video camera for off-line analysis of behavioral seizures. Seizures were graded using a modified Racine scale (Racine, 1972) consisting of Racine stages (RS) III, IV and V, which are considered to reflect the propagation of seizures from forebrain structures (RSIII) to the brainstem (RSV) (Johne et al., 2020; Kellaway and Hrachovy, 1983; Pospelov et al., 2016). The stages were defined as follows: (RSIII) uni- or bilateral forelimb clonus, (RSIV) uni- or bilateral forelimb clonus paralleled by loss of righting reflex and (RSV) tonus-clonus with loss of righting reflex. To qualify for a clonic seizure, unequivocal and uninterrupted clonic jerks with at least 5 repetitions had to be observed. Tonus-clonus was defined as tonic extension of the forelimbs and/or

hindlimbs following clonic seizures or tonic forelimb extension coupled with hindlimb clonus. The observed tonus typically resembled decerebrate rigidity and was often coupled with opisthotonus.

During seizure grading two reviewers, blind to the treatment, recorded latency and duration of each seizure stage. The reported values were agreed on by both reviewers: when disagreements arose, a consensus was reached by discussion.

During mainly the first 10 min after asphyxia, a number of behaviors that were not commonly seen in control animals were observed. These included imbalance, startles, shaking, swimming, pedaling, excessive grooming, kicking, chewing, Straub tail and circling. Some of these behaviors were likely non-convulsive seizures belonging to RSI and II. All of these behaviors were short-lasting, albeit often repetitive, and their presentation varied, which makes their rigorous categorization difficult, and we decided not to include them into the present study (for a detailed description, see Johne *et al.*, 2020).

Freely moving video-electrocorticography

P10-11 rat pups were anesthetized with 4 % isoflurane in room air. After the induction of anesthesia, isoflurane was reduced to 1.5 – 2.5 % and the animal was given 5 mg/kg karprofen (Rimadyl Vet, Pfizer) subcutaneously. The scalp was scrubbed with 100 mg/ml solution of povidone-iodine (Betadine, Takeda) followed by 70 % ethanol before applying 10 % lidocaine solution. A piece of the scalp was removed and cranial windows were drilled over the parietal (A/P -3.8, M/L 2.0 mm from bregma) and the frontal cortex (A/P +1.5, M/L 1.5 mm) for recording electrodes and over the cerebellum (approx. 1 mm caudal from lambda) for a ground electrode. Care was taken to avoid damaging the dura during the drilling. In few (5/27) recordings a second window was drilled over the cerebellum for a reference electrode. 0.8 mm steel screws soldered to a strip connector were placed over the dura. The screws, the connector, the wires and the exposed skull were covered with dental cement. After 30 minutes of recovery on a heating pad, the animals were returned to the litter.

On the day following the surgery, the pups were placed in the asphyxia chamber. A piezo sensor (AB1070B-LW100-R, PUI Audio, Dayton, Ohio, USA) was taped over the flank for recording movement and breathing rhythm. The movement recordings showed a very low contamination of the ECoG recordings (see below; and SVideo 5) by movement artifacts. The electrocorticogram (ECoG) was recorded using extracellular field potential amplifiers (npi EXT-02F/2 [bandwidth 3 – 1300 Hz] and EXT-16DX [0.1 – 500 Hz]; Tamm, Germany). ECoG and piezo signals were digitized at 2 kHz with a Cambridge Electronic Design Micro1401-3 converter (Cambridge, United Kingdom). Most (22/27) recordings were referenced to ground while few

were referenced to the cerebellar reference electrode. After 45 min of baseline recording, the animal was exposed to intermittent asphyxia.

Brain pH/Po_2 and local field potential recordings

In experiments with intracranial recordings, the rat pups were anesthetized with 4 % isoflurane in room air and 1 mg/g urethane was administered intraperitoneally. The animals were transferred on a 35 °C heating plate and isoflurane was reduced to 1.5 – 2.5 % for the surgery. A piece of the scalp was removed and cranial windows were drilled over the parietal cortex (A/P -4.5, M/L 2.5 mm from bregma) for a glass capillary local field potential (LFP) electrode (150 mM NaCl) and over the cerebellum for a Ag/AgCl ground electrode. Additional windows were drilled bilaterally over the parietal cortex (A/P -4.0, M/L 2.0 mm) for pH and Po_2 sensitive microelectrodes (Unisense OX-10 and pH-25, Aarhus, Denmark). To aid fixing the animal, a plastic washer was attached to the skull with a dental cement.

After surgery, isoflurane administration was terminated. The animal was transferred to the recording setup, placed on a heating pad and fixed from the head to a stereotaxic bench. Small-rodent facemask (model OC-MFM, World Precision Instruments, Sarasota, Florida, USA) delivering room air was placed lightly over the snout and a piezo sensor (PMS20, Medifactory, Heerlen, The Netherlands) was taped over the ribcage to record movement and breathing rhythm. Small incisions were cut to the dura for the pH, Po_2 and LFP electrodes and the electrodes were lowered 1 mm into the cerebral cortex. The ground wire was placed over the cerebellum. Rectal temperature was monitored using a RET-4/RET-5 probe and a BAT-12 thermometer (Physitemp, New Jersey, New York, USA). The temperature of the heating pad was adjusted to maintain rectal temperature at approx. 36 °C during the baseline recording. If the animal reacted to a light tail pinch during the setup procedure, an additional 0.25 – 0.5 mg/g urethane was given intraperitoneally.

Details of the recording setup and calibration of pH and Po_2 probes are described in Pospelov *et al.* (2020). After the pH and Po_2 recordings and the animal's rectal temperature had stabilized, 30-60 min after the termination of the isoflurane anesthesia, the baseline recording was started. The animals were then exposed to intermittent asphyxia. To make the recordings comparable to the freely-moving experiments, a dead volume was added in front of the facemask and the gas flow was adjusted to match the slower rate of gas exchange in the chamber using an oximeter (TR250Z 25% oxygen sensor from CO2Meter, Inc. Ormond Beach, Florida USA).

Data analysis and statistics

The statistical analyses were made using Prism v8.0.1 software (Graphpad, San Diego, California, USA) and R v3.6.1. The reported values are median with either 95 % confidence interval (CI) of median or range. The type of variation is explicitly stated on each occasion in the Results. Binary and continuous variables were compared using Barnard's test (Lydersen et al., 2009) and Mann-Whitney U-test, respectively. The difference between groups was considered significant when two-tailed p-value was ≤ 0.05.

Electrographic seizures were manually annotated on bandpass filtered (3-40 Hz) ECoG and LFP recordings. Seizures were defined as abnormal, repetitive spike discharges with an amplitude exceeding baseline mean + 5 * standard deviation and with a duration of ≥ 10 s. Consistent spike bursts occurring less than 10 s (even if shorter than 10 s) before or after the seizure epoch were considered to belong to the same epoch. Annotated electrographic and behavioral seizures were time-synchronized in Spike2 software v9.08 (Cambridge Electronic Design) according to a test light stimulus in the video.

ECoG and LFP power in the 3-40 Hz band was calculated in 30 s windows, adjacent windows separated by 3 s, and normalized to average baseline power. The pH and Po_2 recordings were analysed using custom-made Matlab (MathWorks inv.) scripts as previously described (Pospelov et al., 2020).

RESULTS

Changes in blood pH, base excess and lactate and plasma copeptin evoked by experimental asphyxia

To ascertain the translational relevance of the experimental models used in this work, and to compare the hypoxic burden brought about by the steady and intermittent asphyxia protocols, we measured blood gas parameters which are generally used in the diagnosis of BA. The P11-12 rat pups were exposed to 15 min of steady asphyxia with 5 % O_2 or 30 min of intermittent asphyxia where the O_2 level was altered between 9 % and 5 % in 5 min steps. As in our previous work (Pospelov et al., 2020), CO_2 was kept at 20 % throughout the asphyxia period in both paradigms. We used trunk blood for the analyses.

As expected (see Summanen *et al.*, 2018; Pospelov *et al.*, 2020), both types of asphyxia induced a large decrease in blood pH and base excess (BE) (Fig. 1 A-B). Median pH was 6.81 [95 % confidence interval (CI): 6.80 – 6.87] and 6.93 [6.80 – 6.95], respectively, at the end of steady and intermittent asphyxia; and in the control group at the same time point, 7.53 [7.51 – 7.54]. The acidemia had a prominent metabolic component, as indicated by a fall in BE of 21.2 [18.9 – 22.3] mmol/l and 20.6 [19.3 – 21.2] mmol/l during steady and intermittent protocol, respectively. These BE changes were closely paralleled by an increase in blood lactate from a baseline of 1.1 [1.0 – 1.2] mmol/l under control to 10.9 [8.5 – 14.9] mmol/l and 8.6

[7.0 – 9.8] mmol/l for steady and intermittent asphyxia, respectively (Fig. 1C). In addition, the levels of plasma copeptin, a relevant biomarker of asphyxia (Kelen et al., 2017; Schlapbach et al., 2011), were highly elevated by the end of both asphyxia protocols (4.41 [1.64 – 11.15] nM and 6.32 [4.48 – 7.74] nM for steady and intermittent, respectively vs. 0.22 [0.1 – 2.5] nM in the control group; Fig 1D).

While the duration of the intermittent asphyxia exposure was twice as long as that of steady asphyxia, the blood gas parameters showed quantitatively similar changes. As described in detail before (Pospelov et al., 2020), rat pups have a remarkable ability to physiologically compensate in response to the 9 % O_2 challenge. The near-identical hypoxic burden caused by the two asphyxia protocols is therefore readily explained by the identical total time (15 min) of exposure to 5 % O_2. This similarity is particularly interesting when comparing the efficacy of steady and intermittent asphyxia to induce post-asphyxia seizures, as done below.

Behavioral seizures emerge following intermittent asphyxia, and they are suppressed by Graded Restoration of Normocapnia

We started our experiments on seizure generation in the two asphyxia paradigms using freely moving, non-instrumented rats. Seizure scoring was based on a modified Racine scale (see Methods; Racine, 1972). Accurate, unequivocal scoring of Racine stage I and II (RSI and RSII) behavioral seizures in rat pups is difficult because many of these motor patterns, such as oral movements or automatisms and brief clonic twitches, are often observed also in naive control animals. Thus, to make our results comparable to previous work on models based on pure hypoxia, and as robust as possible for translational work, we excluded RSI and RSII seizures from all quantifications.

Under control conditions, the pups were for most of the time in apparent sleep, often located close to, or touching, the wall of the observation chamber. During the exposure to steady or to intermittent asphyxia, the pups initially displayed distress behavior with increased locomotion, but no seizures were observed. Breathing rate decreased gradually and led to apnea and death in 3/17 and 2/17 pups during exposure to steady and intermittent asphyxia, respectively. There was no further mortality.

Notably, convulsive seizures fulfilling our current criteria (RSIII-V) were never observed after steady asphyxia (see SVideo 1). The pups displayed some abnormal behavior including shaking, twitches and Straub tail during the first 10 minutes of recovery (see also Johne *et al.*, 2020). Thereafter, their behavior became indistinguishable from what was observed under control conditions. The conspicuous lack of seizures following steady asphyxia was not attributable to electroclinical uncoupling (Murray et al., 2008; Scher et al., 2003) as verified in EEG (EcoG) recordings from freely moving animals (data not shown). In

sharp contrast to this, intense behavioral seizures were seen in 7/15 pups shortly after intermittent asphyxia, with a median latency of 224 s [range: 178-310 s] from the end of the exposure (Fig. 2A and SVideo 2-3). Seizures of increasing severity (RSIII-RSV) occurred in succession. They commenced with forelimb clonus (RSIII) which was often coupled with rhythmic head-nodding. This was followed by clonus with loss of righting (RSIV) and the seizures ended after an episode of tonus-clonus with loss of righting in all 7/15 seizing animals (RSV). The median total duration of seizures was 110 s (range: 66-180 s), and all observed seizures terminated within about 8 min after the end of intermittent asphyxia. Seizure termination was followed by a period (typically 40-180 s) of total immobility apart from respiratory movements, after which normal behavior gradually resumed. To our knowledge, this is the first description of a rodent model of human full-term birth asphyxia, in which robust seizures emerge after the termination of the insult, as observed in the NICU (Lynch *et al.*, 2012; and Discussion).

The severe acidosis of the brain that takes place during asphyxia shows a prompt recovery to the alkaline direction after the end of the exposure (see Bender *et al.*, 2003; Pospelov *et al.*, 2020 and Fig. 5). There is evidence indicating that both the amplitude and the rate of alkaline recovery of brain tissue pH, boosts neuronal excitability and the triggering of seizures (Woodbury et al., 1957; Yoshioka et al., 1996). Thus, we examined the efficacy of Graded Restoration of Normocapnia (GRN), a putative therapeutic maneuver which slows down the rate of alkaline recovery (Helmy et al., 2011), in suppressing seizures in the intermittent asphyxia model. We exposed rat pups to the 5 % CO_2 gas for 30 min immediately after intermittent asphyxia. Below, Rapid Restoration of Normocapnia (RRN) refers to the bulk of experiments in which the animals were promptly re-exposed to room air after asphyxia. Indeed, we found that GRN significantly reduced the occurrence of RSIII-V seizures compared to RRN (GRN 2/16 vs. RRN 7/15, p=0.0379 [Barnard's test]; Fig. 2 and SVideo 4). Notably, none of the animals in the GRN group had RSV seizures (p=0.0016 compared to RRN). Thus, GRN reduced both seizure incidence and severity.

Electrocorticographic and behavioral post-asphyxia seizures in freely moving rats

In order to gain insight into the effects of the intermittent asphyxia protocol on neocortical activity patterns and into the relationships between electrographic and behavioral seizures, rat pups were implanted with epidural electrodes over the frontal and the parietal cortex (electrocorticography, ECoG). Before the asphyxia and in control animals, the ECoG was continuous and, characteristic of this age point, discrete bursts of activity were rarely observed (Cirelli and Tononi, 2015; Gramsbergen, 1976) in either recording location (Fig. 3A, excerpt *a*). Immediately following the onset of intermittent asphyxia, the ECoG activity was strongly suppressed. Most of this suppression is attributable to the acidosis caused by the high level (20 %) of CO_2 as will be demonstrated below (Figs. 4 and 5). Nevertheless, as shown in Fig. 3A (lower panel), during the initial phase of the asphyxia with 9 % of O_2 about 25 % of the activity persisted as quantified by

ECoG power while the subsequent fall to 5 % O_2 led to a further decrease with hardly any detectable activity. These effects were remarkably constant during the three transitions from 9 % to 5 % O_2 in the intermittent asphyxia protocol (Fig. 3A, lower panel and excerpt *b-c*).

In line with the purely behavioral observations in Fig. 2, we never observed electrographic seizure activity during the asphyxia exposure. In contrast, the ECoG recordings showed intense post-asphyxia seizure activity in 6 out of 10 freely-behaving animals which is in excellent agreement with the seizure incidence described above (Fig. 2) in the non-instrumented animals. The electrographic seizures were observed over the parietal cortex with a median latency of 150 [95% CI: 108-188] s after the end of asphyxia. In all animals the electrographic seizures appeared practically simultaneously at the recording sites in the parietal and the frontal cortex. The spread of the post-asphyxia seizures over large cortical areas is an interesting and important observation, which implies that our 2-site recording is sufficient for reliable neocortical seizure detection in the present model.

Most of the seizures consisted of spike trains with a 1.2-2.3 Hz discharge frequency (see Fig. 3B for an example). The spike amplitudes increased towards the end of the seizure epoch. Small changes (range: -0.6 to 0.6 Hz) in discharge frequency were observed during the seizure epochs, but they did not follow any consistent pattern. While ECoG bursts in the initial seizure period (Fig 3B, excerpt *a*) were monopolar without 3 Hz high-pass filtering, we did not see slow components in the full-blown epileptiform spikes (Fig 3B, excerpt *b*). The seizures terminated very abruptly (change from high amplitude spiking to complete cessation of epileptiform activity occurred within 0-7 s), after which the ECoG signal at both recording sites fell to a low level with hardly any detectable activity. Thereafter, baseline activity gradually recovered.

The ECoG recordings demonstrated a consistent temporal overlap between the RSIII-V behavioral seizures and the electrographic seizures (Fig. 3B-C), but there was no clear change in the ECoG upon transition from one RSIII-V stage to another (SVideo 5). The ECoG seizures preceded the RSIII-V behavioral seizures by 19 to 71 s. During this time, abnormal behavior, such as shaking, twitches and Straub tail, was observed. Most of these aberrant behaviors were likely non-convulsive seizures belonging to the RSI-RSII categories, which were excluded from our analyses (see Methods and Johne *et al.*, 2020). After this period of initial electroclinical uncoupling, RSIII-V seizures emerged after a delay in all animals which had electrographic seizures. Thus, behavioral scoring of RSIII-V seizures provides a valid method for seizure detection in the present model. In 4/6 cases, RSV seizures, which are considered to originate from the brainstem (Kellaway and Hrachovy, 1983; Pospelov et al., 2016), continued for an additional 3-13 s after the cortical seizures had terminated (Fig. 3C).

GRN decreased the post-asphyxia seizure incidence from 6/10 to 3/10 as seen in both behavior and ECoG. In agreement with the data on freely moving non-instrumented animals (Fig. 2A), RSV seizures were absent in the instrumented GRN group as well (Fig. 2B). Otherwise, the seizures were qualitatively similar to those observed after RRN: behavioural seizures appeared after parietal and frontal ECoG seizures and outlasted the electrographic seizures in 2/3 animals or (1/3) were terminated simultaneously. No spontaneous behavioural or electrographic seizures were observed in the control group (n=7).

Simultaneous recording of neocortical LFPs, brain pH and brain oxygen levels during intermittent asphyxia

While the data presented in Fig. 3 show that changes in ambient CO_2 and O_2 exert robust effects on neuronal excitability over a wide scale (from profound suppression to hyperexcitability during and after intermittent asphyxia, respectively), they provide no information on the relative contributions of the associated changes in brain pH and brain Po_2 (Pospelov et al., 2020). Therefore, we made simultaneous recordings of local-field potential (LFP) activity and pH as well as Po_2 from the parietal cortex in head-fixed urethane-anesthetized rats. While urethane is known to suppress seizures (Cain et al., 1992), the dose used presently (see Methods) had a partial inhibitory action only, thus enabling a meaningful analysis of the dependence of neuronal activity on pH and O_2 during and after asphyxia.

The sample recording in Fig. 4 shows the quality of the raw data. Exposure to intermittent asphyxia (with the initial 9 % O_2) caused a fast decline in brain pH, and the ongoing LFP activity, and the three shifts in ambient O_2 from 9 % to 5 % produced a further, reversible suppression (cf. Figs. 3 and 5). A major decrease in Po_2 was caused only by the three exposures to 5 % O_2. A prompt increase in neuronal excitability took place leading to seizure activity within 2.8 min post-asphyxia in a manner comparable to what was seen in freely moving animals (Fig. 3). Moreover, the seizure pattern was similar, consisting of epileptiform spikes with a crescendo pattern.

Suppression of LFP activity during intermittent asphyxia is mainly attributable to the fall in brain pH

Simultaneous recordings of LFP, pH and *P*o2 were done in a total of 29 animals: LFP and Po_2 recordings were recorded from 16-17 and 12 animals in the RRN and GRN group, respectively, whereas pH was available from 14 animals in the RRN group and 7 animals in the GRN group. LFP power within 3-40 Hz band was used in order to quantify neuronal activity throughout these experiments (Fig. 5).

During the first 5 min of intermittent asphyxia (with 9 % O_2), the median value of brain pH (RRN and GRN groups combined) decreased rapidly from 7.33 to 6.95 (Fig. 5B), with a further decline to 6.78 during the

next 5 min in 5 % O_2 (Fig. 5; see gray and white vertical columns below protocol scheme across traces in A-C). pH recovered only slightly (0.12 units; less than 20 % of the maximum acidosis) in response to the two subsequent 9 % O_2 bouts, and dropped below 6.7 during the second and third 5 % O_2 exposures, reaching a minimum of 6.67.

Median brain Po_2 during the pre-asphyxia baseline was 30.0 mmHg. During the first 5 min period of intermittent asphyxia with 9 % O_2, brain Po_2 showed initially a small transient fall (nadir at 22 mmHg; cf. Fig. 4), but promptly recovered back to the baseline level, *indicating a fast re-establishment of brain normoxia* despite the large fall in ambient O_2 (Fig. 5C). Notably, however, under these conditions, median LFP power was still suppressed to 10 % [95 % CI: 8.3 % – 11 %] from its baseline level, in agreement with the high level of acidosis. A similar recovery to brain normoxia, associated with a strong suppression of LFP when compared to baseline (to 16 % [13 % – 19 %]), was observed during the two subsequent exposures to 9 % O_2. In contrast to the brain normoxia achieved during the 9 % O_2 exposures, all three epochs with 5 % O_2 during the intermittent asphyxia led to a decrease in brain Po_2 to a level where virtually no free oxygen could be detected. Under these conditions, LFP activity was – consistent with the associated acid shift – further suppressed, but not totally abolished, retaining 4.1 % [3.3 % – 5.1 %] of the baseline power (see magnified power trace in Fig. 5A). Thus, all the above data indicate that the LFP power was suppressed by up to 90 % despite normoxic conditions within the brain at 9 % ambient O_2 because the major factor influencing neuronal excitability during the intermittent asphyxia protocol is the simultaneous hypercapnic acidosis.

Dependence of the post-asphyxia increase in neuronal excitability and seizures on brain pH changes

After RRN, brain pH recovered in a biphasic manner, apparently reflecting the different elimination rates of CO_2 and lactacidosis (Pospelov et al., 2020). During the initial, fast phase which had a duration of 5 min (in a time window of 2.0-7.0 min after the end of asphyxia), brain pH increased from 6.75 to 7.26 at a maximal rate of 0.29 pH units/min (Fig. 5B and inset *b* therein). This was followed by an almost linear and much slower (0.0086 pH units/min) secondary recovery phase lasting until 15 min post-asphyxia. We did not observe an alkaline overshoot of the kind described in P6 rats with steady asphyxia induced by 9 % O_2 and 20 % CO_2 (Helmy et al., 2012, 2011), suggesting that fast brain pH recovery in itself is sufficient in triggering seizures following asphyxia (see also Panaitescu *et al.*, 2018).

As expected, GRN reduced the rate of the fast phase of brain pH recovery after intermittent asphyxia. The median time required to reach the pH level at the end of the fast phase in the RRN group was 5 min and, following GRN, 13 min. The rate of pH recovery during the subsequent slower phase with GRN was closely similar to what was observed after RRN, but it took place at a more acidotic level with its start set by the

slower rate of the preceding fast phase. The full recovery of brain pH following GRN had a third, final phase which was caused by the change from 5% ambient CO_2 to room air, and was completed within 10 min.

Following RRN, there was a prompt increase in neuronal activity. In 12/16 animals this was followed by the emergence of recurring spike bursts (single burst duration <10 s) which in three cases transformed into prominent seizures (duration 94-117 s). Thus, while the median LFP power rapidly exceeded the baseline level reaching an apex 2.4 times higher than baseline power, the peak power of individual LFP recordings showed large variation ranging from 1.3-71 x [baseline power] (Fig. 5A and inset *a* therein), with a their peaks at around 3.5 – 4.5 min after the asphyxia. When compared to freely moving animals, the lower incidence of clear-cut seizure activity in experiments of the kind illustrated in Figs. 4 and 5 is readily explained by the use of urethane anesthesia. Regardless, a period of hyperexcitability, coinciding with the fast phase of pH recovery (2.0-7.0 min after the asphyxia), was consistently associated with RRN (Fig. 5A inset *a*). In contrast to this, in the GRN experiments the median LFP power returned to the baseline level promptly after the asphyxia but no significant overshoot was observed. Accordingly, the median LFP power during the fast phase of pH recovery was significantly higher in the RRN than in the GRN group (p=0.0130 [Mann-Whitney U-test]; RRN 1.5 [95% CI: 1.1-3.3], GRN 1.1 [95% CI: 0.75-1.5]).

A striking conclusion which emerges from the present data is that, while seizures are clearly generated only at pH levels relatively close to baseline (> 7.0), it is not only the absolute pH but also *the rate of change of pH within a defined pH window* which is tightly linked to the triggering of seizures. This conclusion is supported by the astonishingly accurate temporal overlap of the massive (RRN) and slight (GRN) increases in LFP power seen during the 2-7 min window after the asphyxia (Fig. 5A inset *a*). The corresponding estimates for the maximum rate of brain pH change during RRN and GRN are 0.29 pH-units/min and 0.23 pH-units/min, respectively (Fig. 5B inset *b*).

Absence of effect of brain O_2 on seizure generation after intermittent asphyxia

When the animals in the RRN group were re-exposed to room air after asphyxia, median brain Po_2 recovered rapidly (max 140 mmHg/min at 1 min) with an overshoot to 85 mmHg (cf. 30.0 mm Hg during baseline) at 2.0 min after the end of the intermittent asphyxia (Fig. 5C). Brain Po_2 fell to the baseline level 6.6 min later and continued to gradually decline until it reached 16.4 mmHg 26 min after asphyxia. Thereafter, it begun to slowly increase. When the experiment was terminated 90 min after the end of asphyxia, brain Po_2 had recovered to 23 mmHg. GRN had no effect on the rate (max 146 mmHg/min) or magnitude (apex 88 mmHg) of the brain Po_2 overshoot. However, GRN increased the duration of the overshoot: median Po_2 remained elevated for the whole 30 min period of 5 % CO_2 application. Thereafter, the RRN and GRN Po_2 curves merged. It is noteworthy that brain Po_2 in both the GRN and the RRN group is

well above baseline at the time when seizures emerge. Taken together, our data show beyond any doubt that post-asphyxia seizures are not triggered by brain hypoxia, which is, again, consistent with birth-asphyxia seizures seen in human neonates (Lynch et al., 2012).

DISCUSSION

In this study, we used our P11-12 rat model of human term birth asphyxia to explore the basic mechanisms of BA-induced behavioral convulsions and neocortical electrographic seizures. In a recent study on brain-sparing mechanisms in this model (Pospelov et al., 2020), post-asphyxia hyperexcitability and seizures were blocked by a slightly lower experimental temperature (34 vs 36 °C) (cf. Tooley *et al.*, 2003 and Bennet *et al.*, 2007). The developmental stage of the cortex of P11-12 rats is comparable to the human term neonate (Clancy et al., 2007; Romijn et al., 1991; Semple et al., 2013), and the asphyxia insult in our model targets the whole organism akin to the situation during parturition. This is true also for the fetal sheep umbilical cord occlusion model which has yielded an enormous amount of translationally relevant information (Drury et al., 2015; Hassell et al., 2015). In contrast to the widely-used invasive rodent model by Rice, Vannucci and Brierley (Rice *et al.*, 1981; see also Vannucci & Vannucci, 2005), in which unilateral ligation of the common carotid artery is followed by exposure to pure hypoxia, the present rodent model preserves the organism's innate physiological responses to asphyxia, including CO_2-dependent vasoactive mechanisms (Boedtkjer, 2018; Giussani, 2016; Lear et al., 2018) and other brain-protective mechanisms, such as the hormonal responses triggered during birth (Evers and Wellmann, 2016; Spoljaric et al., 2017).

Hypercapnia is an endogenous seizure-suppressing factor during the asphyxia-linked hypoxia

Asphyxia is, by definition, a combination of hypercapnia and hypoxia. Hypercapnic acidosis of the brain leads to suppression of neuronal activity as is evident in the ECoG and LFP recordings in Figs 3-5 (Dulla et al., 2005; Lee et al., 1996; Lennox, 1936; Mitchell and Grubbs, 1956; Pollock, 1949; Tolner et al., 2011; Ziemann et al., 2008), while alkalosis has the opposite effect (Dulla et al., 2005; Lee et al., 1996; Lennox, 1936; Nasreddine et al., 2020; Schuchmann et al., 2011, 2006). Indeed, a wide variety of neuronal ion channels, which control intrinsic neuronal excitability and synaptic signaling, show a high and functionally synergistic sensitivity to pH (Pasternack et al., 1996; Spray et al., 1981; Tombaugh and Somjen, 1997; Traynelis and Cull-Candy, 1990; Wemmie et al., 2013; Wilkins et al., 2005), which suggests that the suppression of excitability by acidosis during asphyxia is deeply rooted in mammalian evolution (see Ruusuvuori & Kaila, 2014). An obvious corollary of the above is that the protective actions of exogenous CO_2 observed in invasive models with pure-hypoxia exposure (e.g. Vannucci *et al.*, 1995, 1997, 2001) simply mimic the effects of the endogenous hypercapnia, which are always associated with BA. In contrast to this, in current rodent models of BA and/or HIE which are based on exposure of rat and mouse pups to pure

hypoxia induced by a gas mixture with a low O_2 (typically 4-8 % O_2 in N_2) (Greggio et al., 2009; Jensen et al., 1991; Rakhade et al., 2011; Rodriguez-Alvarez et al., 2015; Zanelli et al., 2014; Zayachkivsky et al., 2015), seizures are triggered already *during* the insult. Moreover, pure hypoxia (which does not occur under real-life physiological or pathophysiological conditions) evokes an immediate brain-confined alkalosis (Pospelov et al., 2020), which is exactly the opposite of what happens during asphyxia. Moreover, the electrographic seizures seen after asphyxia have initially a low amplitude (Figs. 3 and 4; Johne et al, 2020), while neocortical seizures induced by pure hypoxia start with a high amplitude of the epileptiform spikes, followed by a gradual decay (Cleary et al., 2013; Jensen et al., 1991; Rakhade et al., 2011; Talos et al., 2013). All these salient differences between the present BA model and the pure-hypoxia models point to the involvement of distinct seizure-promoting mechanisms, which is obviously of high relevance when considering the translational validity of these models. Most importantly, the behavioral and neocortical seizures in our model are triggered only *after* the BA-mimicking insult, which is consistent with the fact that seizures in human neonates are typically observed *after*, but not during, asphyxic birth (Lynch et al., 2012).

Post-asphyxia seizure generation depends on the rate of pH recovery after asphyxia

The convulsive behavioral seizures seen after intermittent asphyxia were closely paralleled by neocortical seizures as demonstrated by ECoG recordings. The electrographic seizures consisted of epileptiform spikes, with a frequency roughly similar to those seen in rat pups during hyperthermia-induced brain alkalosis (Ruusuvuori et al., 2013; Schuchmann et al., 2006). They commenced with a relatively low initial amplitude, followed by a subsequent increase towards the end of the discharge. The seizure discharges had a duration of 77-151 s (n=6), and ended abruptly. As noted above, a rise in pH is known to enhance neuronal excitability and to facilitate seizures. In line with this, both the incidence and severity of the seizures seen after RRN were strongly reduced by GRN (a procedure that slows down the net efflux of CO_2 from the brain), which in the present work was achieved by application of 5 % CO_2 in room air at the start of the recovery period. With GRN, the incidence of RSIII and RSIV seizures decreased from 7/15 to 2/16 and 1/16 animals, respectively, and no RSV seizures were seen at all.

The strong dependence of post-asphyxia hyperexcitability and seizures on pH recovery was directly demonstrated in simultaneous recordings of cortical pH, Po_2 and LFP activity done under light urethane anesthesia. In these experiments, a prominent period of post-asphyxia hyperexcitability took place, during which some animals (3/16) developed frank seizures (Fig. 5). The time window of hyperexcitability and seizures coincided with the fast post-asphyxia recovery of brain pH and, again, GRN led to a near-complete abolishment of post-asphyxia hyperexcitability. Thus, all our behavioral and electrophysiological data are consistent with the idea that the post-asphyxia seizure generation is triggered in response to the rapid rise in brain pH. The onset of enhanced excitability is observed at a time point when the brain is still acidotic,

suggesting that both the absolute brain pH level and the rate of the increase in pH are critical parameters involved in the establishment of the post-asphyxia hyperexcitability. Notably, the rates of recovery of brain Po_2 were similar following GRN and RRN, indicating a lack of contribution of the rate of the O_2 increase to the suppression of seizure propensity following GRN. These data demonstrate that GRN is an effective seizure-suppressing maneuver with a much lower CO_2 level (5 %) than what was previously tested in a P7 rat model (10 % in Helmy *et al.*, 2011). Moreover, it is obvious that a much briefer duration (around 10 min, given the seizure time window of 2-7 min post-asphyxia) than the pre-set time of 30 min for the present experiments would have been sufficient for the anticonvulsant action (cf. Figs 3-5).

Post-asphyxia seizures are not strictly related to the preceding hypoxic load

Strikingly, the intermittent – but not the steady – asphyxia protocol gave rise to pronounced behavioral seizures spanning the whole Racine scale (up to grade V in 7/15 rats), which were tightly associated with electrographic neocortical seizures. Because our aim was to develop a robust seizure model for future research on putative novel therapeutic strategies, we did not include non-convulsive seizure behaviors (RSI-II) in the present analyses (for detailed scoring of such seizures in the present model, see Johne *et al.*, 2020). Notably, both asphyxia protocols led to changes in blood gas parameters which fulfill the main diagnostic criteria of human BA: an acidemia with a decrease in pH below 7.0, coupled to a fall in base excess by 20 mmol/l and elevation of lactate by about 10 mmol/l. The massive release of copeptin (a stable fragment of prepro-AVP) to blood, which is triggered by the hypoxia component of asphyxia (Summanen et al., 2018), provides further support for the validity of our present model (Kelen et al., 2017; Schlapbach et al., 2011).

The above data on blood acid-base parameters indicate that the post-asphyxia hyperexcitability and seizure generation are not strictly related to the magnitude of hypoxic load. Thus, while the intermittent asphyxia protocol resulted in severe behavioral post-asphyxia seizures (RSIII-V) in about half of the animals tested, we never observed seizures following steady asphyxia. Moreover, the post-asphyxia seizures can be readily evoked by an intermittent paradigm in which the 9 % and 5 % 0_2 bouts have a duration of 7 and 3 min, respectively (Johne et al., 2020), instead of the current 5-and-5 min paradigm.

The observation that intermittent -- but not steady -- asphyxia with a varying level of O_2 was able to trigger seizures, cannot be mechanistically explained by our current data. A possible scenario that might account for the efficacy of intermittent asphyxia in triggering seizures is that mechanisms, which have been shown to promote anoxic/hypoxic LTP *in vitro* (Di Filippo et al., 2008; Hsu and Huang, 1997; Quintana et al., 2015), are likely to be activated during the 5 % O_2 bouts of intermittent asphyxia. The enhanced network activity during the periods with 9 % O_2 (and transient brain normoxia) would then lead to further potentiation of

excitatory connections. Finally, during the recovery from asphyxia, the suppressing effect of the hypercapnic acidosis is quickly removed, unmasking the enhanced excitability, which results in seizure generation.

Conclusions

We demonstrate here for the first time behavioral convulsions and neocortical electrographic seizures which are generated in a rat model that physiologically mimics birth asphyxia in human full-term neonates. Notably, these seizures show a critical dependence on brain CO_2/pH. Of course, we do not argue that brain pH changes would be the most important factor in all kinds of post-asphyxia seizures in human neonates. These seizures are likely to be mechanistically heterogeneous between and even within individuals, as is evident from EEG recordings and from the highly variable (and usually inadequate) therapeutic responses to standard anticonvulsant agents (Boylan et al., 2019; Connell et al., 1989; Lloyd et al., 2017; Shellhaas and Clancy, 2007; van Rooij et al., 2013). In fact, while much work on rodent models has focused on neuronal molecules and signaling mechanism that are *affected* as a *consequence* of seizures (Lippman-Bell et al., 2016; Rakhade et al., 2011; Sun et al., 2013; Wang et al., 2011; Zhou et al., 2015), next to nothing is known about the *proximate causes in vivo* which are responsible for rendering the neonate brain prone to seizures after BA. Given the steep dependence of neuronal excitability on brain pH, it is reasonable to assume that the large pH changes which take place during and following birth asphyxia in human neonates (Uria-Avellanal and Robertson, 2014) are likely to contribute to the multiple mechanisms that lead to the generation of post-asphyxia seizures.

Using an inhaled gas mixture with elevated (5 %) CO_2 might be difficult in the NICU, especially when fast decisions regarding therapeutic interventions have to be made (Soul et al., 2019). Therefore, additional strategies targeting post-asphyxia changes in brain pH (Uria-Avellanal and Robertson, 2014) should be examined in future work. Our present study (see also Pospelov *et al.*, 2020) also calls for much more attention on the post-partum control of systemic CO_2 (Kro et al., 2013). Clearly, aggressive resuscitation of asphyxiated neonates, aiming at a maximally fast recovery to normoxia will lead to hypocapnia, which is a well-known general risk factor for poor outcome, and is likely to promote seizures via brain pH-dependent effects (Uria-Avellanal and Robertson, 2014).

ACKNOWLEDGEMENTS

We thank Merle Kampura for assistance in the molecular biological analyses, and Maria Partanen, Madara Snepere and Ann-Christine Aho for the breeding and maintaining of the experimental

animals. This work was supported by Grant ERC-2013-AdG 341116 (KK) and the Jane and Aatos Erkko foundation (KK).

CONFLICT OF INTEREST

The authors declare that they have no conflict of interest.

REFERENCES

Ahearne, C.E., Boylan, G.B., Murray, D.M., 2016. Short and long term prognosis in perinatal asphyxia: An update. World J. Clin. Pediatr. 5, 67–74. https://doi.org/10.5409/wjcp.v5.i1.67

American Academy of Pediatrics, American College of Obstetricians and Gynecologists, 2014. Neonatal Encephalopathy and Neurologic Outcome, Second Edition. Pediatrics 133, e1482–e1488. https://doi.org/10.1542/peds.2014-0724

Bender, T.M., Johnston, J.A., Manepalli, A.N., Mink, R.B., 2003. Association between brain tissue pH and brain injury during asphyxia in piglets. Resuscitation 59, 243–254. https://doi.org/10.1016/S0300-9572(03)00207-7

Bennet, L., Dean, J.M., Wassink, G., Gunn, A.J., 2007. Differential Effects of Hypothermia on Early and Late Epileptiform Events After Severe Hypoxia in Preterm Fetal Sheep. J. Neurophysiol. 97, 572–578. https://doi.org/10.1152/jn.00957.2006

Bittigau, P., Sifringer, M., Genz, K., Reith, E., Pospischil, D., Govindarajalu, S., Dzietko, M., Pesditschek, S., Mai, I., Dikranian, K., Olney, J.W., Ikonomidou, C., 2002. Antiepileptic drugs and apoptotic neurodegeneration in the developing brain. Proc. Natl. Acad. Sci. 99, 15089–15094. https://doi.org/10.1073/pnas.222550499

Boedtkjer, E., 2018. Acid–base regulation and sensing: Accelerators and brakes in metabolic regulation of cerebrovascular tone. J. Cereb. Blood Flow Metab. 38, 588–602. https://doi.org/10.1177/0271678X17733868

Boylan, G.B., Kharoshankaya, L., Mathieson, S.R., 2019. Diagnosis of seizures and encephalopathy using conventional EEG and amplitude integrated EEG, 1st ed, Handbook of Clinical Neurology. Elsevier B.V. https://doi.org/10.1016/B978-0-444-64029-1.00018-7

Cain, D.P., Boon, F., Hargreaves, E.L., 1992. Evidence for different neurochemical contributions to long-term potentiation and to kindling and kindling-induced potentiation: Role of NMDA and urethane-sensitive mechanisms. Exp. Neurol. 116, 330–338. https://doi.org/10.1016/0014-4886(92)90011-E

Cirelli, C., Tononi, G., 2015. Cortical development, electroencephalogram rhythms, and the sleep/wake cycle. Biol. Psychiatry 77, 1071–1078. https://doi.org/10.1016/j.biopsych.2014.12.017

Clancy, B., Finlay, B.L., Darlington, R.B., Anand, K.J.S., 2007. Extrapolating brain development from experimental species to humans. Neurotoxicology 28, 931–937. https://doi.org/10.1016/j.neuro.2007.01.014

Cleary, R.T., Sun, H., Huynh, T., Manning, S.M., Li, Y., Rotenberg, A., Talos, D.M., Kahle, K.T., Jackson, M.,

Rakhade, S.N., Berry, G., Jensen, F.E., 2013. Bumetanide Enhances Phenobarbital Efficacy in a Rat Model of Hypoxic Neonatal Seizures. PLoS One 8, 1–12. https://doi.org/10.1371/journal.pone.0057148

Connell, J., Oozeer, R., de Vries, L., Dubowitz, L.M.S., Dubowitz, V., 1989. Clinical and EEG response to anticonvulsants in neonatal seizures. Arch. Dis. Child. 64, 459–464. https://doi.org/10.1136/adc.64.4_Spec_No.459

Dalman, C., Thomas, H. V., David, A.S., Gentz, J., Lewis, G., Allebeck, P., 2001. Signs of asphyxia at birth and risk of schizophrenia Population-based case—control study. Br. J. Psychiatry 179, 403–408. https://doi.org/10.1192/bjp.179.5.403

Di Filippo, M., Tozzi, A., Costa, C., Belcastro, V., Tantucci, M., Picconi, B., Calabresi, P., 2008. Plasticity and repair in the post-ischemic brain. Neuropharmacology 55, 353–362. https://doi.org/10.1016/j.neuropharm.2008.01.012

Drury, P.P., Bennet, L., Booth, L.C., Davidson, J.O., Wassink, G., Gunn, A.J., 2015. Studies of Perinatal Asphyxial Brain Injury in the Fetal Sheep, in: Animal Models of Neurodevelopmental Disorders. pp. 85–105. https://doi.org/10.1007/978-1-4939-2709-8_7

Dulla, C.G., Dobelis, P., Pearson, T., Frenguelli, B.G., Staley, K.J., Masino, S.A., 2005. Adenosine and ATP link PCO2to cortical excitability via pH. Neuron 48, 1011–1023. https://doi.org/10.1016/j.neuron.2005.11.009

Evers, K.S., Wellmann, S., 2016. Arginine Vasopressin and Copeptin in Perinatology. Front. Pediatr. 4, 2–11. https://doi.org/10.3389/fped.2016.00075

Giussani, D.A., 2016. The fetal brain sparing response to hypoxia: Physiological mechanisms. J. Physiol. 594, 1215–1230. https://doi.org/10.1113/JP271099

Glass, H.C., Glidden, D., Jeremy, R.J., Barkovich, A.J., Ferriero, D.M., Miller, S.P., 2009. Clinical Neonatal Seizures are Independently Associated with Outcome in Infants at Risk for Hypoxic-Ischemic Brain Injury. J. Pediatr. 155, 318–323. https://doi.org/10.1016/j.jpeds.2009.03.040

Gramsbergen, A., 1976. The development of the EEG in the rat. Dev. Psychobiol. 9, 501–515. https://doi.org/10.1002/dev.420090604

Greggio, S., Rosa, R.M., Dolganov, A., de Oliveira, I.M., Menegat, F.D., Henriques, J.A.P., DaCosta, J.C., 2009. NAP prevents hippocampal oxidative damage in neonatal rats subjected to hypoxia-induced seizures. Neurobiol. Dis. 36, 435–444. https://doi.org/10.1016/j.nbd.2009.08.008

Hassell, K.J., Ezzati, M., Alonso-Alconada, D., Hausenloy, D.J., Robertson, N.J., 2015. New horizons for newborn brain protection: Enhancing endogenous neuroprotection. Arch. Dis. Child. Fetal Neonatal Ed. 100, F541–F551. https://doi.org/10.1136/archdischild-2014-306284

Helmy, M.M., Ruusuvuori, E., Watkins, P. V., Voipio, J., Kanold, P.O., Kaila, K., 2012. Acid extrusion via blood-brain barrier causes brain alkalosis and seizures after neonatal asphyxia. Brain 135, 3311–3319. https://doi.org/10.1093/brain/aws257

Helmy, M.M., Tolner, E.A., Vanhatalo, S., Voipio, J., Kaila, K., 2011. Brain alkalosis causes birth asphyxia seizures, suggesting therapeutic strategy. Ann. Neurol. 69, 493–500. https://doi.org/10.1002/ana.22223

Hsu, K.S., Huang, C.C., 1997. Characterization of the anoxia-induced long-term synaptic potentiation in area CA1 of the rat hippocampus. Br. J. Pharmacol. 122, 671–81. https://doi.org/10.1038/sj.bjp.0701409

Ikonomidou, C., Turski, L., 2010. Antiepileptic drugs and brain development. Epilepsy Res. 88, 11–22. https://doi.org/10.1016/j.eplepsyres.2009.09.019

Jensen, F.E., Applegate, C.D., Holtzman, D., Belin, T.R., Burchfiel, J.L., 1991. Epileptogenic effect of hypoxia in the immature rodent brain. Ann. Neurol. 29, 629–637. https://doi.org/10.1002/ana.410290610

Jensen, F.E., Wang, C., 1996. Hypoxia-induced hyperexcitability in vivo and in vitro in the immature hippocampus. Epilepsy Res. 26, 131–140. https://doi.org/10.1016/S0920-1211(96)00049-6

Johne, M., Römermann, K., Hampel, P., Gailus, B., Theilmann, W., Ala-Kurikka, T., Kaila, K., Löscher, W., 2020. Phenobarbital and midazolam suppress neonatal seizures in a novel rat model of term birth asphyxia while bumetanide is ineffective manuscript.

Kawasaki, K., Traynelis, S.F., Dingledine, R., 1990. Different responses of CA1 and CA3 regions to hypoxia in rat hippocampal slice. J. Neurophysiol. 63, 385–394. https://doi.org/10.1152/jn.1990.63.3.385

Kelen, D., Andorka, C., Szabó, M., Alafuzoff, A., Kaila, K., Summanen, M., 2017. Serum copeptin and neuron specific enolase are markers of neonatal distress and long-term neurodevelopmental outcome. PLoS One 12, 1–11. https://doi.org/10.1371/journal.pone.0184593

Kellaway, P., Hrachovy, R.A., 1983. Status epilepticus in newborns: a perspective on neonatal seizures. Adv Neurol 34, 93–99.

Kharoshankaya, L., Stevenson, N.J., Livingstone, V., Murray, D.M., Murphy, B.P., Ahearne, C.E., Boylan, G.B., 2016. Seizure burden and neurodevelopmental outcome in neonates with hypoxic–ischemic encephalopathy. Dev. Med. Child Neurol. 58, 1242–1248. https://doi.org/10.1111/dmcn.13215

Kro, G.A.B., Yli, B.M., Rasmussen, S., Rosén, K.G., Amer-Wåhlin, I., Stray-Pedersen, B., Saugstad, O.D., 2013. Association between umbilical cord artery pCO2 and the Apgar score; Elevated levels of pCO2 may be beneficial for neonatal vitality after moderate acidemia. Acta Obstet. Gynecol. Scand. 92, 662–670. https://doi.org/10.1111/aogs.12090

Lagercrantz, H., 2016. The good stress of being born. Acta Paediatr. 105, 1413–1416. https://doi.org/10.1111/apa.13615

Lawn, J.E., Cousens, S., Zupan, J., 2005. Neonatal Survival 1 4 million neonatal deaths : When ? Where ? Why ? Lancet 9–18. https://doi.org/10.1016/S0140-6736(05)71048-5

Lear, C.A., Wassink, G., Westgate, J.A., Nijhuis, J.G., Ugwumadu, A., Galinsky, R., Bennet, L., Gunn, A.J., 2018. The peripheral chemoreflex: indefatigable guardian of fetal physiological adaptation to labour. J. Physiol. 596, 5611–5623. https://doi.org/10.1113/JP274937

Lee, J., Taira, T., Pihlaja, P., Ransom, B.R., Kaila, K., 1996. Effects of CO2 on excitatory transmission apparently caused by changes in intracellular pH in the rat hippocampal slice. Brain Res. 706, 210–216. https://doi.org/10.1016/0006-8993(95)01214-1

Lennox, W.G., 1936. Effect on the electroencephalogram of drugs and conditions which influence seizures. Arch. Neurol. Psychiatry 36, 1236. https://doi.org/10.1001/archneurpsyc.1936.02260120083006

Lippman-Bell, J.J., Zhou, C., Sun, H., Feske, J.S., Jensen, F.E., 2016. Early-life seizures alter synaptic calcium-

permeable AMPA receptor function and plasticity. Mol. Cell. Neurosci. 76, 11–20. https://doi.org/10.1016/j.mcn.2016.08.002

Lloyd, R.O., O'Toole, J.M., Pavlidis, E., Filan, P.M., Boylan, G.B., 2017. Electrographic Seizures during the Early Postnatal Period in Preterm Infants. J. Pediatr. 187, 18-25.e2. https://doi.org/10.1016/j.jpeds.2017.03.004

Lydersen, S., Fagerland, M.W., Laake, P., 2009. Recommended tests for association in 2×2 tables. Stat. Med. 28, 1159–1175. https://doi.org/10.1002/sim.3531

Lynch, N.E., Stevenson, N.J., Livingstone, V., Murphy, B.P., Rennie, J.M., Boylan, G.B., 2012. The temporal evolution of electrographic seizure burden in neonatal hypoxic ischemic encephalopathy. Epilepsia 53, 549–557. https://doi.org/10.1111/j.1528-1167.2011.03401.x

McBride, M.C., Laroia, N., Guillet, R., 2000. Electrographic seizures in neonates correlate with poor neurodevelopmental outcome. Neurology 55, 506–514. https://doi.org/10.1212/WNL.55.4.506

Miller, S.P., Weiss, J., Barnwell, A., Ferriero, D.M., Latal-Hajnal, B., Ferrer-Rogers, A., Newton, N., Partridge, J.C., Glidden, D. V., Vigneron, D.B., Barkovich, A.J., 2002. Seizure-associated brain injury in term newborns with perinatal asphyxia. Neurology 58, 542–548. https://doi.org/10.1212/WNL.58.4.542

Mitchell, W.G., Grubbs, R.C., 1956. Inhibition of Audiogenic Seizures by Carbon Dioxide. Science (80-.). 123, 223–224. https://doi.org/10.1126/science.123.3189.223

Modabbernia, A., Mollon, J., Boffetta, P., Reichenberg, A., 2016. Impaired Gas Exchange at Birth and Risk of Intellectual Disability and Autism: A Meta-analysis. J. Autism Dev. Disord. 46, 1847–1859. https://doi.org/10.1007/s10803-016-2717-5

Murray, D.M., Boylan, G.B., Ali, I., Ryan, C.A., Murphy, B.P., Connolly, S., 2008. Defining the gap between electrographic seizure burden, clinical expression and staff recognition of neonatal seizures. Arch. Dis. Child. Fetal Neonatal Ed. 93, 187–192. https://doi.org/10.1136/adc.2005.086314

Nasreddine, W., Fakhredin, M., Makke, Y., Hmaimess, G., Sabbagh, S., Beaini, S., El Tourjuman, O., Beydoun, A., 2020. Hyperventilation-induced high-amplitude rhythmic slowing: A mimicker of absence seizures in children. Epilepsy Behav. 103, 106510. https://doi.org/10.1016/j.yebeh.2019.106510

Panaitescu, A.M., Isac, S., Pavel, B., Ilie, A.S., Ceanga, M., Totan, A., Zagrean, L., Peltecu, G., Zagrean, A.M., 2018. Oxytocin reduces seizure burden and hippocampal injury in a rat model of perinatal asphyxia. Acta Endocrinol. (Copenh). 14, 315–319. https://doi.org/10.4183/aeb.2018.315

Pappas, A., Korzeniewski, S.J., 2016. Long-Term Cognitive Outcomes of Birth Asphyxia and the Contribution of Identified Perinatal Asphyxia to Cerebral Palsy. Clin. Perinatol. 43, 559–572. https://doi.org/10.1016/j.clp.2016.04.012

Pasternack, M., Voipio, J., Kaila, K., 1996. Proton modulation of functionally distinct GABAA receptors in acutely isolated pyramidal neurons of rat hippocampus. Neuropharmacology 35, 1279–1288. https://doi.org/10.1111/j.1748-1716.1993.tb09553.x

Peng, B.W., Justice, J.A., He, X.H., Sanchez, R.M., 2013. Decreased A-currents in hippocampal dentate granule cells after seizure-inducing hypoxia in the immature rat. Epilepsia 54, 1223–1231. https://doi.org/10.1111/epi.12150

Perez, R., Espinoza, M., Riquelme, R., Parer, J.T., Llanos, A.J., 1989. Arginine vasopressin mediates

cardiovascular responses to hypoxemia in fetal sheep. Am. J. Physiol. Integr. Comp. Physiol. 256, R1011–R1018. https://doi.org/10.1152/ajpregu.1989.256.5.R1011

Pollock, G.H., 1949. CENTRAL INHIBITORY EFFECTS OF CARBON DIOXIDE: I. Felis domesticus. J. Neurophysiol. 12, 315–324. https://doi.org/10.1152/jn.1949.12.5.315

Pospelov, A.S., Puskarjov, M., Kaila, K., Voipio, J., 2020. Endogenous brain-sparing responses in brain pH and P O2 in a rodent model of birth asphyxia. Acta Physiol. 0–3. https://doi.org/10.1111/apha.13467

Pospelov, A.S., Yukin, A.Y., Blumberg, M.S., Puskarjov, M., Kaila, K., 2016. Forebrain-independent generation of hyperthermic convulsions in infant rats. Epilepsia 57, e1–e6. https://doi.org/10.1111/epi.13230

Pressler, R.M., Lagae, L., 2019. Why we urgently need improved seizure and epilepsy therapies for children and neonates. Neuropharmacology 107854. https://doi.org/10.1016/j.neuropharm.2019.107854

Pressler, R.M., Mangum, B., 2013. Newly emerging therapies for neonatal seizures. Semin. Fetal Neonatal Med. 18, 216–223. https://doi.org/10.1016/j.siny.2013.04.005

Quintana, P., Soto, D., Poirot, O., Zonouzi, M., Kellenberger, S., Muller, D., Chrast, R., Cull-Candy, S.G., 2015. Acid-sensing ion channel 1a drives AMPA receptor plasticity following ischemia and acidosis in hippocampal CA1 neurons. J. Physiol. 19, 1–32. https://doi.org/10.1113/JP270701

Racine, R.J., 1972. Modification of seizure activity by electrical stimulation: II. Motor seizure. Electroencephalogr. Clin. Neurophysiol. 32, 281–294. https://doi.org/10.1016/0013-4694(72)90177-0

Rainaldi, M.A., Perlman, J.M., 2016. Pathophysiology of Birth Asphyxia. Clin. Perinatol. 43, 409–422. https://doi.org/10.1016/j.clp.2016.04.002

Rakhade, S.N., Klein, P.M., Huynh, T., Hilario-Gomez, C., Kosaras, B., Rotenberg, A., Jensen, F.E., 2011. Development of later life spontaneous seizures in a rodent model of hypoxia-induced neonatal seizures. Epilepsia 52, 753–765. https://doi.org/10.1111/j.1528-1167.2011.02992.x

Rice, J.E., Vannucci, R.C., Brierley, J.B., 1981. The influence of immaturity on hypoxic-ischemic brain damage in the rat. Ann. Neurol. 9, 131–141. https://doi.org/10.1002/ana.410090206

Rodriguez-Alvarez, N., Jimenez-Mateos, E.M., Dunleavy, M., Waddington, J.L., Boylan, G.B., Henshall, D.C., 2015. Effects of hypoxia-induced neonatal seizures on acute hippocampal injury and later-life seizure susceptibility and anxiety-related behavior in mice. Neurobiol. Dis. 83, 100–114. https://doi.org/10.1016/j.nbd.2015.08.023

Romijn, H.J., Hofman, M.J., Gransbergen, A., 1991. At what age is the developing cortex of the rat comparable to that of the full term newborn baby? Early Hum.Dev. 26, 61–67.

Rosso, I.M., Cannon, T.D., Huttunen, T., Huttunen, M.O., Lönnqvist, J., Gasperoni, T.L., 2000. Obstetric risk factors for early-onset schizophrenia in a Finnish birth cohort. Am. J. Psychiatry 157, 801–807. https://doi.org/10.1176/appi.ajp.157.5.801

Ruusuvuori, E., Huebner, A.K., Kirilkin, I., Yukin, A.Y., Blaesse, P., Helmy, M., Kang, H.J., El Muayed, M., Hennings, J.C., Voipio, J., Šestan, N., Hübner, C.A., Kaila, K., 2013. Neuronal carbonic anhydrase VII provides GABAergic excitatory drive to exacerbate febrile seizures. EMBO J. 32, 2275–2286. https://doi.org/10.1038/emboj.2013.160

Ruusuvuori, E., Kaila, K., 2014. Carbonic Anhydrases and Brain pH in the Control of Neuronal Excitability, in: Sub-Cellular Biochemistry. pp. 271–290. https://doi.org/10.1007/978-94-007-7359-2_14

Sampath, D., White, A.M., Raol, Y.H., 2014. Characterization of neonatal seizures in an animal model of hypoxic-ischemic encephalopathy. Epilepsia 55, 985–993. https://doi.org/10.1111/epi.12646

Sanders, R.D., Manning, H.J., Robertson, N.J., Ma, D., Edwards, A.D., Hagberg, H., Maze, M., 2010. Preconditioning and postinsult therapies for perinatal hypoxic-ischemic injury at term. Anesthesiology 113, 233–249. https://doi.org/10.1097/ALN.0b013e3181dc1b84

Saugstad, O.D., Oei, J.L., Lakshminrusimha, S., Vento, M., 2019. Oxygen therapy of the newborn from molecular understanding to clinical practice. Pediatr. Res. 85, 20–29. https://doi.org/10.1038/s41390-018-0176-8

Scher, M.S., Alvin, J., Gaus, L., Minnigh, B., Painter, M.J., 2003. Uncoupling of EEG-clinical neonatal seizures after antiepileptic drug use. Pediatr. Neurol. 28, 277–280. https://doi.org/10.1016/S0887-8994(02)00621-5

Schlapbach, L.J., Frey, S., Bigler, S., Manh-Nhi, C., Aebi, C., Nelle, M., Nuoffer, J.M., 2011. Copeptin concentration in cord blood in infants with early-onset sepsis, chorioamnionitis and perinatal asphyxia. BMC Pediatr 11, 38. https://doi.org/10.1186/1471-2431-11-38

Schuchmann, S., Hauck, S., Henning, S., Grüters-Kieslich, A., Vanhatalo, S., Schmitz, D., Kaila, K., 2011. Respiratory alkalosis in children with febrile seizures. Epilepsia 52, 1949–1955. https://doi.org/10.1111/j.1528-1167.2011.03259.x

Schuchmann, S., Schmitz, D., Rivera, C., Vanhatalo, S., Salmen, B., Mackie, K., Sipilä, S.T., Voipio, J., Kaila, K., 2006. Experimental febrile seizures are precipitated by a hyperthermia-induced respiratory alkalosis. Nat. Med. 12, 823. https://doi.org/10.1038/nm1422

Semple, B.D., Blomgren, K., Gimlin, K., Ferriero, D.M., Noble-Haeusslein, L.J., 2013. Brain development in rodents and humans: Identifying benchmarks of maturation and vulnerability to injury across species. Prog. Neurobiol. 106–107, 1–16. https://doi.org/10.1016/j.pneurobio.2013.04.001

Shellhaas, R.A., Clancy, R.R., 2007. Characterization of neonatal seizures by conventional EEG and single-channel EEG. Clin. Neurophysiol. 118, 2156–2161. https://doi.org/10.1016/j.clinph.2007.06.061

Shi, X.Y., Hu, L.Y., Liu, M.J., Zou, L.P., 2017. Hypercapnia-induced brain acidosis: Effects and putative mechanisms on acute kainate induced seizures. Life Sci. 176, 82–87. https://doi.org/10.1016/j.lfs.2017.03.018

Soul, J.S., Pressler, R., Allen, M., Boylan, G., Rabe, H., Portman, R., Hardy, P., Zohar, S., Romero, K., Tseng, B., Bhatt-Mehta, V., Hahn, C., Denne, S., Auvin, S., Vinks, A., Lantos, J., Marlow, N., Davis, J.M., 2019. Recommendations for the design of therapeutic trials for neonatal seizures. Pediatr. Res. 85, 943–954. https://doi.org/10.1038/s41390-018-0242-2

Spoljaric, A., Seja, P., Spoljaric, I., Virtanen, M.A., Lindfors, J., Uvarov, P., Summanen, M., Crow, A.K., Hsueh, B., Puskarjov, M., Ruusuvuori, E., Voipio, J., Deisseroth, K., Kaila, K., 2017. Vasopressin excites interneurons to suppress hippocampal network activity across a broad span of brain maturity at birth. Proc. Natl. Acad. Sci. 201717337. https://doi.org/10.1073/pnas.1717337114

Spray, D., Harris, A., Bennett, M., 1981. Gap junctional conductance is a simple and sensitive function of intracellular pH. Science (80-.). 211, 712–715. https://doi.org/10.1126/science.6779379

Summanen, M., Bäck, S., Voipio, J., Kaila, K., 2018. Surge of Peripheral Arginine Vasopressin in a Rat Model of Birth Asphyxia. Front. Cell. Neurosci. 12, 1–9. https://doi.org/10.3389/fncel.2018.00002

Sun, H., Juul, H.M., Jensen, F.E., 2016. Models of hypoxia and ischemia-induced seizures. J. Neurosci. Methods 260, 252–260. https://doi.org/10.1016/j.jneumeth.2015.09.023

Sun, H., Kosaras, B., Klein, P.M., Jensen, F.E., 2013. Mammalian target of rapamycin complex 1 activation negatively regulates Polo-like kinase 2-mediated homeostatic compensation following neonatal seizures. Proc. Natl. Acad. Sci. U. S. A. 110, 5199–204. https://doi.org/10.1073/pnas.1208010110

Talos, D.M., Chang, M., Kosaras, B., Fitzgerald, E., Murphy, A., Folkerth, R.D., Jensen, F.E., 2013. Antiepileptic effects of levetiracetam in a rodent neonatal seizure model. Pediatr. Res. 73, 24–30. https://doi.org/10.1038/pr.2012.151

Tolner, E.A., Hochman, D.W., Hassinen, P., Otáhal, J., Gaily, E., Haglund, M.M., Kubová, H., Schuchmann, S., Vanhatalo, S., Kaila, K., 2011. Five percent CO2 is a potent, fast-acting inhalation anticonvulsant. Epilepsia 52, 104–114. https://doi.org/10.1111/j.1528-1167.2010.02731.x

Tombaugh, G.C., Somjen, G.G., 1997. Differential sensitivity to intracellular pH among high- and low-threshold Ca2+ currents in isolated rat CA1 neurons. J. Neurophysiol. 77, 639–653. https://doi.org/10.1152/jn.1997.77.2.639

Tooley, J.R., Satas, S., Porter, H., Silver, I.A., Thoresen, M., 2003. Head cooling with mild systemic hypothermia in anesthetized piglets is neuroprotective. Ann. Neurol. 53, 65–72. https://doi.org/10.1002/ana.10402

Traynelis, S.F., Cull-Candy, S.G., 1990. Proton inhibition of N-methyl-D-aspartate receptors in cerebellar neurons. Nature 345, 347–350. https://doi.org/10.1038/345347a0

Uria-Avellanal, C., Robertson, N.J., 2014. Na+/H+ Exchangers and Intracellular pH in Perinatal Brain Injury. Transl. Stroke Res. 5, 79–98. https://doi.org/10.1007/s12975-013-0322-x

van Rooij, L.G.M., Hellström-Westas, L., De Vries, L.S., 2013. Treatment of neonatal seizures. Semin. Fetal Neonatal Med. 18, 209–215. https://doi.org/10.1016/j.siny.2013.01.001

van Rooij, L.G.M., Toet, M.C., van Huffelen, A.C., Groenendaal, F., Laan, W., Zecic, A., de Haan, T., van Straaten, I.L.M., Vrancken, S., van Wezel, G., van der Sluijs, J., ter Horst, H., Gavilanes, D., Laroche, S., Naulaers, G., de Vries, L.S., 2010. Effect of Treatment of Subclinical Neonatal Seizures Detected With aEEG: Randomized, Controlled Trial. Pediatrics 125, e358–e366. https://doi.org/10.1542/peds.2009-0136

Vannucci, R.C., Brucklacher, R.M., Vannucci, S.J., 1997. Effect of Carbon Dioxide on Cerebral Metabolism during Hypoxia-Ischemia in the Immature Rat. Pediatr. Res. 42, 24–29. https://doi.org/10.1203/00006450-199707000-00005

Vannucci, R.C., Towfighi, J., Brucklacher, R.M., Vannucci, S.J., 2001. Effect of Extreme Hypercapnia on Hypoxic-Ischemic Brain Damage in the Immature Rat. Pediatr. Res. 49, 799–803. https://doi.org/10.1203/00006450-200106000-00015

Vannucci, R.C., Towfighi, J., Heitjan, D.F., Brucklacher, R.M., 1995. Carbon dioxide protects the perinatal brain from hypoxic- ischemic damage: an experimental study in the immature rat. Pediatrics 95, 868–874.

Vannucci, R.C., Vannucci, S.J., 2005. Perinatal hypoxic-ischemic brain damage: Evolution of an animal model. Dev. Neurosci. 27, 81–86. https://doi.org/10.1159/000085978

Vutskits, L., 2014. Cerebral blood flow in the neonate. Paediatr. Anaesth. 24, 22–29. https://doi.org/10.1111/pan.12307

Wang, Y., Zhan, L., Zeng, W., Li, K., Sun, W., Xu, Z.C., Xu, E., 2011. Downregulation of hippocampal GABA after hypoxia-induced seizures in neonatal rats. Neurochem. Res. 36, 2409–2416. https://doi.org/10.1007/s11064-011-0565-4

Wellmann, S., Benzing, J., Cippà, G., Admaty, D., Creutzfeldt, R., Mieth, R.A., Beinder, E., Lapaire, O., Morgenthaler, N.G., Haagen, U., Szinnai, G., Bührer, C., Bucher, H.U., 2010. High copeptin concentrations in umbilical cord blood after vaginal delivery and birth acidosis. J. Clin. Endocrinol. Metab. 95, 5091–5096. https://doi.org/10.1210/jc.2010-1331

Wemmie, J.A., Taugher, R.J., Kreple, C.J., 2013. Acid-sensing ion channels in pain and disease. Nat. Rev. Neurosci. 14, 461–471. https://doi.org/10.1038/nrn3529

Wilkins, M.E., Hosie, A.M., Smart, T.G., 2005. Proton modulation of recombinant GABAA receptors: Influence of GABA concentration and the β subunit TM2-TM3 domain. J. Physiol. 567, 365–377. https://doi.org/10.1113/jphysiol.2005.088823

Wirrell, E.C., Armstrong, E.A., Osman, L.D., Yager, J.Y., 2001. Prolonged seizures exacerbate perinatal hypoxic-ischemic brain damage. Pediatr. Res. 50, 445–454. https://doi.org/10.1203/00006450-200110000-00005

Woodbury, D.M., Rollins, L.T., Gardner, M.D., Hirschi, W.L., Hogan, J.R., Rallison, M.L., Tanner, G.S., Brodie, D.A., 1957. Effects of Carbon Dioxide on Brain Excitability and Electrolytes. Am. J. Physiol. Content 192, 79–90. https://doi.org/10.1152/ajplegacy.1957.192.1.79

Yoshioka, H., Nioka, S., Miyake, H., Zaman, A., Sawada, T., Chance, B., 1996. Seizure susceptibility during recovery from hypercapnia in neonatal dogs. Pediatr. Neurol. 15, 36–40. https://doi.org/10.1016/0887-8994(96)00116-6

Zanelli, S., Goodkin, H.P., Kowalski, S., Kapur, J., 2014. Impact of transient acute hypoxia on the developing mouse EEG. Neurobiol. Dis. https://doi.org/10.1016/j.nbd.2014.03.005

Zanelli, S.A., Rajasekaran, K., Grosenbaugh, D.K., Kapur, J., 2015. Increased excitability and excitatory synaptic transmission during in vitro ischemia in the neonatal mouse hippocampus. Neuroscience. https://doi.org/10.1016/j.neuroscience.2015.09.046

Zayachkivsky, A., Lehmkuhle, M.J., Ekstrand, J.J., Dudek, F.E., 2015. Ischemic injury suppresses hypoxia-induced electrographic seizures and the background EEG in a rat model of perinatal hypoxic-ischemic encephalopathy. J. Neurophysiol. 114, 2753–2763. https://doi.org/10.1152/jn.00796.2014

Zhou, C., Sun, H., Klein, P.M., Jensen, F.E., 2015. Neonatal seizures alter NMDA glutamate receptor GluN2A and 3A subunit expression and function in hippocampal CA1 neurons. Front. Cell. Neurosci. 9, 1–11. https://doi.org/10.3389/fncel.2015.00362

Ziemann, A.E., Schnizler, M.K., Albert, G.W., Severson, M.A., Howard, M.A., Welsh, M.J., Wemmie, J.A., 2008. Seizure termination by acidosis depends on ASIC1a. Nat. Neurosci. 11, 816–822. https://doi.org/10.1038/nn.2132

FIGURE CAPTIONS

FIGURE 1. Changes in blood pH **(A)**, base excess **(B)** lactate **(C)**, and plasma copeptin **(D)** in P11-12 rats exposed to experimental asphyxia. The line graphs on the top illustrate the intermittent and steady asphyxia protocols. Both protocols decreased pH to < 7.0 and BE by 20 mmol/l (ΔBE), and evoked a marked increase in lactate and copeptin. The vertical grey bar marks the end of asphyxia, and, for clarity, the blue symbols have been shifted slightly to the left and the brown symbols slightly to the right. The values are median with 95 % CIs. All data are based on P11-P12 rats in this and subsequent figures.

FIGURE 2. Incidence of Racine stage III-V behavioral seizures after experimental asphyxia. **(A)** Freely moving, non-instrumented rats were exposed to steady or intermittent asphyxia followed by rapid (RRN) or graded restoration of normocapnia (GRN). No seizures were seen after steady asphyxia, whereas they were triggered in 7/15 animals after intermittent asphyxia with RRN. GRN significantly decreased the proportion of animals with RSIII-IV seizures and abolished RSV seizures. **(B)** Similar to (A) but the animals had been implanted with epidural, cortical electrodes 24 h earlier (see Fig. 3 for electrocorticography). GRN abolished RSV seizures also in these experiments.

FIGURE 3. Electrographic and behavioral seizures emerge after but not during intermittent asphyxia. **(A)** Experimental design and the effect of asphyxia on cortical activity. The panels on the left show the gas application protocol (top), an example of a frontal electrocorticography (ECoG) recording (middle) and median power [95 % CI] of 18 frontal ECoG recordings (bottom). Excerpts *a-c* marked on the example ECoG are shown on the right. These data demonstrate a profound suppression of cortical activity during asphyxia. The placements of electrodes are shown in the illustration on the lower right corner. **(B)** An example of a post-asphyxia recording (asphyxia ends at time 0) showing the temporal relationship between behavioral and electrographic seizures. Top panel shows the behavioral seizure stages and middle and bottom panels show frontal and parietal ECoG, respectively. Excerpts *a* and *b* from the frontal ECoG displaying the early and the late parts of the seizures are shown in the lower left corner. We included two frequency bands to show the seizure activity appears without possible filtering artefacts. (C) Timeline representation of all ECoG (frontal and parietal) seizures and behavioral seizures in the RRN group. The recording marked by an asterisk is the same as in (B).

FIGURE 4. A sample recording with simultaneous monitoring of parietal cortex local field potentials (LFP), as well as brain pH and Po_2. After the intermittent asphyxia, prominent seizure activity was seen in the LFP recording (top panel). Excerpt of the LFP trace (marked with *a*) including the seizure epoch is shown below in blue. Middle and bottom panels show the pH and Po_2 recordings, respectively. To facilitate visual

inspection, the three gray vertical columns mark the 9 % O_2 bouts during the intermittent asphyxia protocol.

FIGURE 5. Changes in cortical activity (A) and in brain pH (B) and Po_2 (C) in rat pups exposed to intermittent asphyxia, followed by rapid (RRN) or graded restoration of normocapnia (GRN). All values are median [95 % CI] except for panel A inset *a* (on the right). The three vertical grey columns on data panels mark the 9% O_2 bouts during the intermittent protocol whereas the two vertical lines indicate the end of asphyxia and the end of GRN. Median data for the RRN and GRN protocols are plotted separately starting at 2 min after the end of asphyxia as the conditions before this time point are identical in the two protocols. **(A)** Power of local field potentials (LFPs) in the parietal cortex. The trace with a separate y-axis is a six-fold magnification of the LFP power and shows the profound suppression of cortical activity during asphyxia (cf. Fig. 4). After asphyxia, the activity recovers promptly. Following RRN, but not GRN, a period of hyperexcitability and seizures was seen, and it coincided with the rapid alkaline recovery of brain pH during a time window of 2 to 7 min after the end of asphyxia. The inset shows individual LFP power traces during this period. **(B)** Brain pH decreases by 0.6 pH-units during the asphyxia and displays only minor modulation (0.12 pH-units) upon the changes between the 9% and 5% O_2 levels. The alkaline recovery of brain pH after RRN is biphasic, and it is slowed down by GRN. The brain pH during the first recovery phase (2-7 min) is shown magnified in insest *b*. **(C)** Brain Po_2 falls to apparent zero during the three periods of exposure to 5 % O_2, but recovers to achieve a normoxic level when the ambient O_2 level is increased to 9 % O_2. After the asphyxia, an overshoot of *P*o2 is observed. GRN increases the duration but not the amplitude or rate of the *P*o2 overshoot.

FIGURE 1

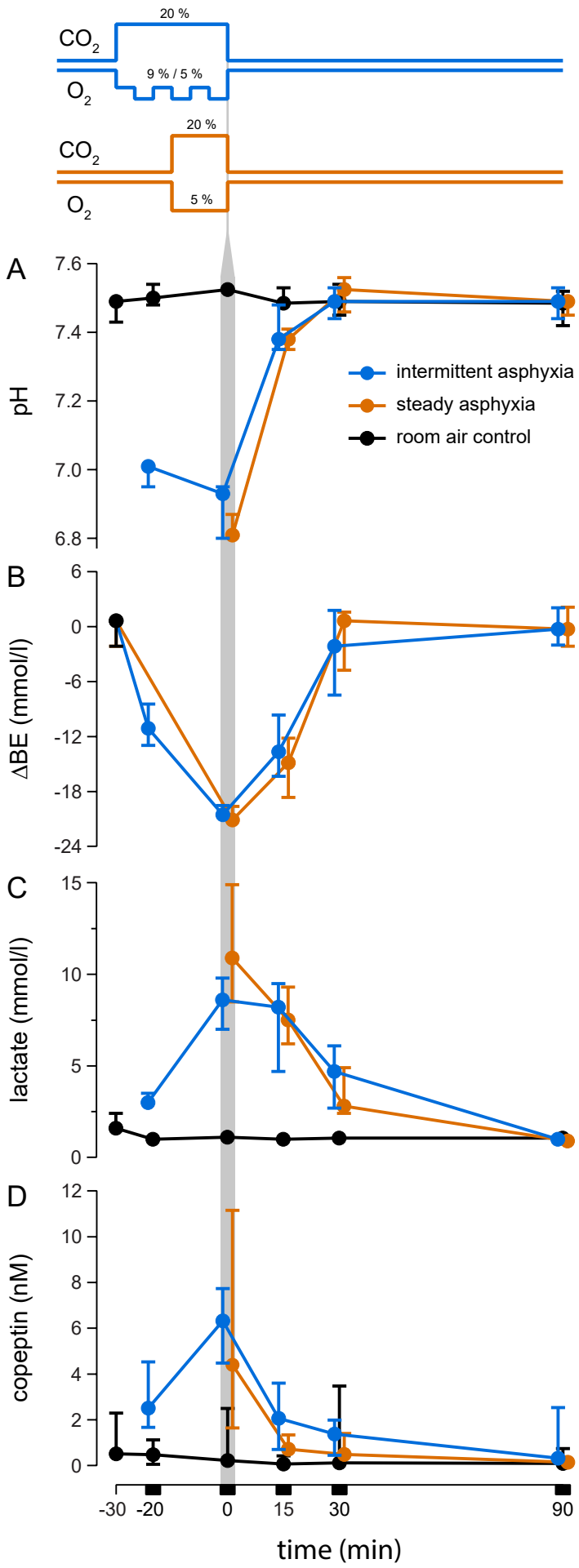
20 %
CO2
9 % / 5 %
O2
20 %
CO2
5 %
O2
A
pH
7.6
7.4
7.2
7.0
6.8
intermittent asphyxia
steady asphyxia
room air control
B
ΔBE (mmol/l)
6
0
-6
-12
-18
-24
C
lactate (mmol/l)
15
10
5
0
D
copeptin (nM)
12
10
8
6
4
2
0
-30
-20
0
15
30
90
time (min)

FIGURE 2

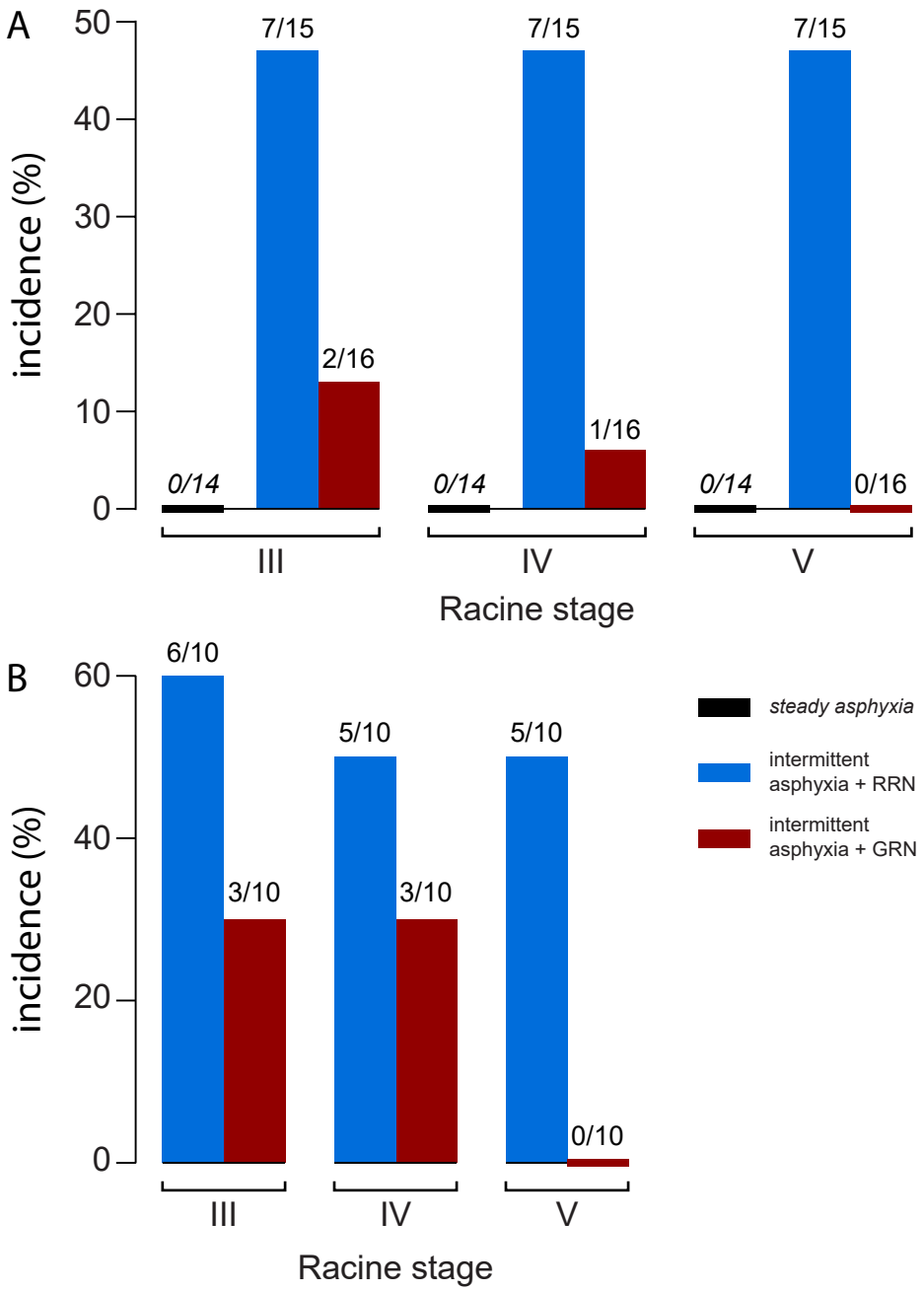
A
incidence (%)
50
40
30
20
10
0
7/15
2/16
7/15
1/16
7/15
0/16
0/14
0/14
0/14
III
IV
V
Racine stage
B
incidence (%)
60
40
20
0
6/10
3/10
5/10
3/10
5/10
0/10
III
IV
V
Racine stage
steady asphyxia
intermittent asphyxia + RRN
intermittent asphyxia + GRN

FIGURE 3

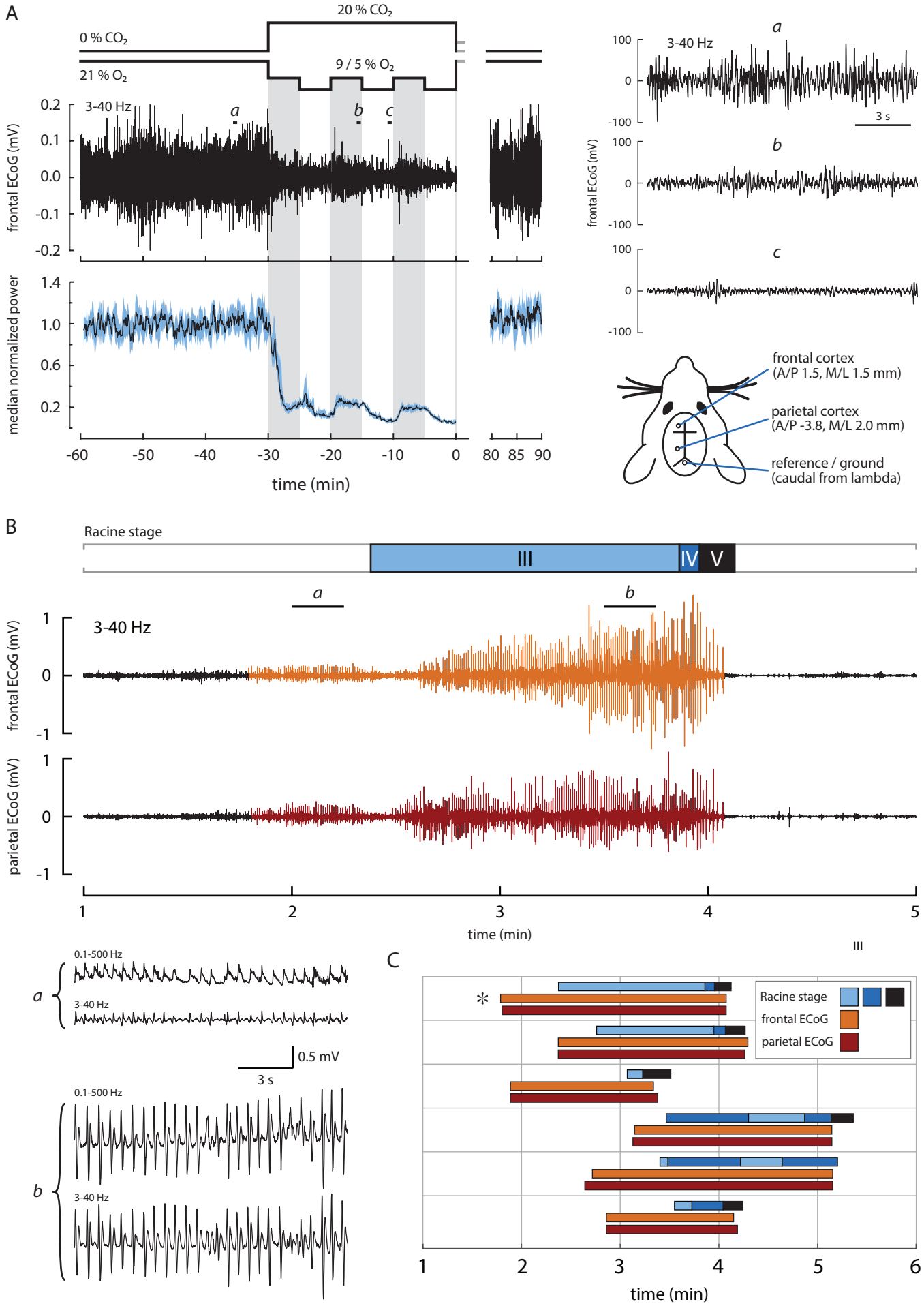
A
20 % CO2
0 % CO2
9 / 5 % O2
21 % O2
3-40 Hz
a
b
c
frontal ECoG (mV)
median normalized power
time (min)
3 s
frontal cortex
(A/P 1.5, M/L 1.5 mm)
parietal cortex
(A/P -3.8, M/L 2.0 mm)
reference / ground
(caudal from lambda)
B
Racine stage
III
IV
V
parietal ECoG (mV)
0.1-500 Hz
0.5 mV
C
Racine stage
frontal ECoG
parietal ECoG

FIGURE 4

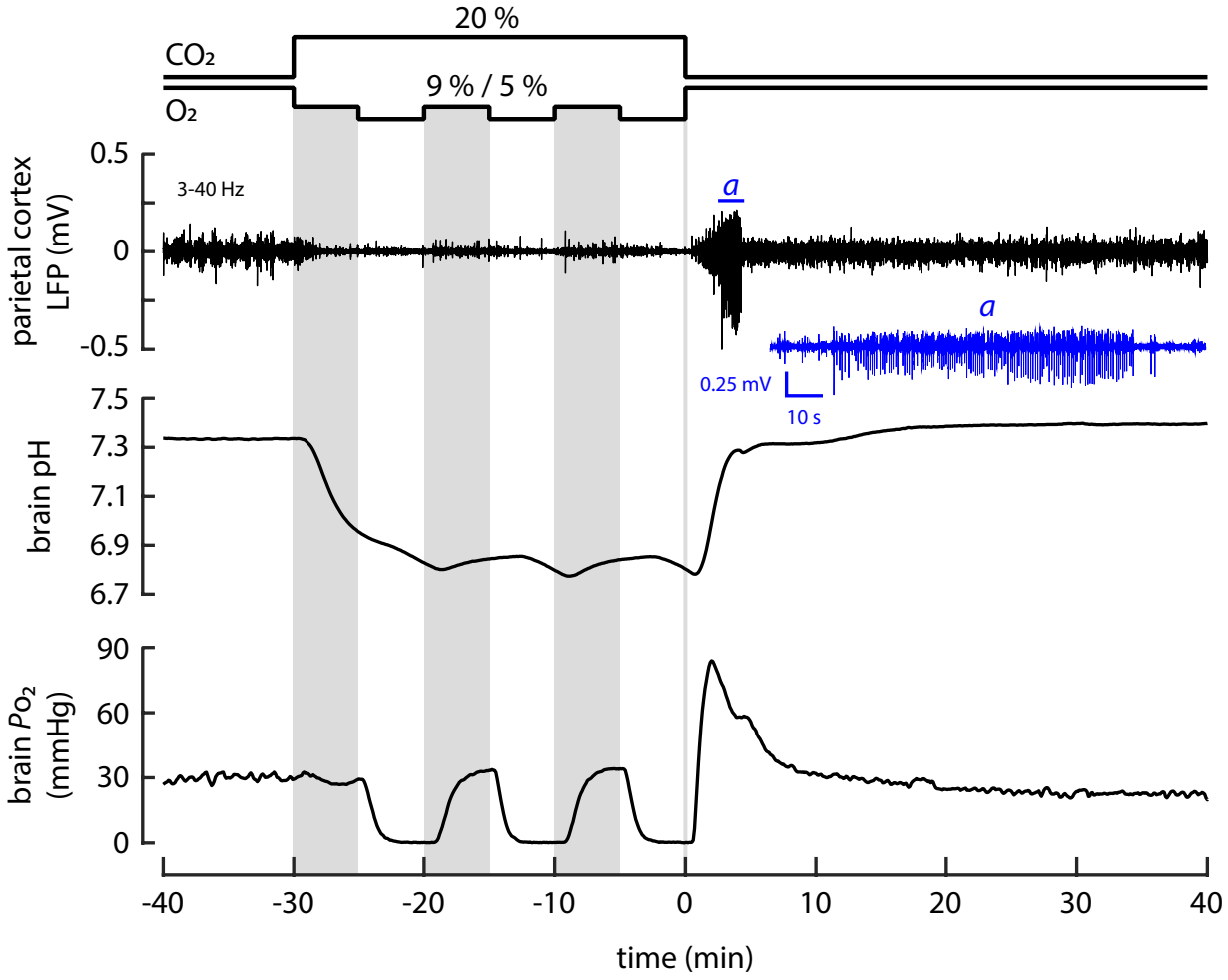
20 %
CO2
9 % / 5 %
O2
parietal cortex
LFP (mV)
0.5
0
-0.5
3-40 Hz
a
a
0.25 mV
10 s
brain pH
7.5
7.3
7.1
6.9
6.7
brain Po2
(mmHg)
90
60
30
0
-40
-30
-20
-10
0
10
20
30
40
time (min)

FIGURE 5

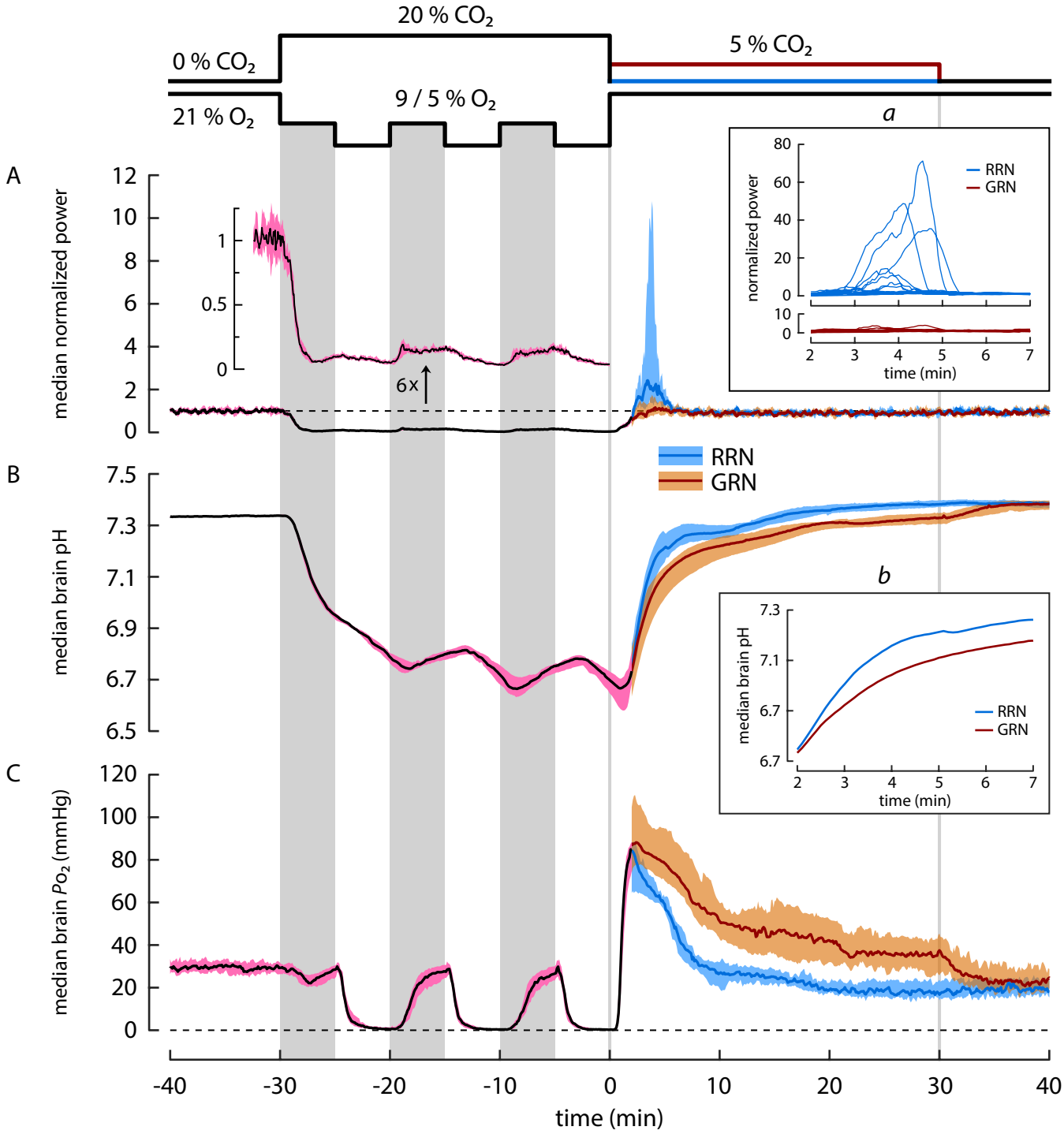
20 % CO2
0 % CO2
5 % CO2
9 / 5 % O2
21 % O2
A
median normalized power
6x
a
normalized power
RRN
GRN
time (min)
B
median brain pH
RRN
GRN
b
median brain pH
RRN
GRN
time (min)
C
median brain Po2 (mmHg)
time (min)